Analysing the Effect of Stoping Parameters on Stability of Decline: Malanjkhand Copper Project, HCL

Dissertation submitted to
Visvesvaraya National Institute of Technology, Nagpur
in partial fulfillment of the requirements for the award of
the degree

Master of Technology
in
Excavation Engineering

By

Gadamalla Rahul (MT23EXV001)

under the guidance of

Dr. Sumant Mohanto **Dr. Nikhil Ninad Sirdesai**

Department of Mining Engineering
Visvesvaraya National Institute of Technology
Nagpur 440 010 (India)

June 2025

Analysing the Effect of Stoping Parameters on Stability of Decline: Malanjkhand Copper Project, HCL

Dissertation submitted to
Visvesvaraya National Institute of Technology, Nagpur
in partial fulfillment of the requirements for the award of
the degree

Master of Technology
in
Excavation Engineering

by

Gadamalla Rahul (MT23EXV001)

under the guidance of

Dr. Sumant Mohanto **Dr. Nikhil Ninad Sirdesai**

Department of Mining Engineering
Visvesvaraya National Institute of Technology
Nagpur 440 010 (India)

June 2025

© Visvesvaraya National Institute of Technology (VNIT)

Department of Mining Engineering
Visvesvaraya National Institute of Technology
Nagpur

Declaration

I, **Gadamalla Rahul**, hereby declare that this dissertation titled **"Analysing the Effect of Stoping Parameters on Stability of Decline: Malanjkhand Copper Project, HCL"** is carried out by me in the Department of Mining Engineering of Visvesvaraya National Institute of Technology, Nagpur. The work is original and has not been submitted earlier whole or in part for the award of any degree/diploma at this or any other Institution / University.

Name and signature
Date:

Department of Mining Engineering
Visvesvaraya National Institute of Technology
Nagpur

Certificate

This is to certify that the dissertation titled **"Analysing the Effect of Stoping Parameters on Stability of Decline: Malanjkhand Copper Project, HCL"** is submitted by **Gadamalla Rahul** in partial fulfillment of the requirements for the award of the degree of **Master of Technology in Excavation Engineering**, VNIT Nagpur. The work is comprehensive, complete, and fit for final evaluation.

Dr. Sumant Mohanto
Supervisor
Assistant Professor,
Department of Mining Engineering,
VNIT, Nagpur

Dr. Nikhil Ninad Sirdesai
Co-Supervisor
Assistant Professor,
Department of Mining Engineering,
VNIT, Nagpur

Dr. Ajay Kumar Agarwal
Head, Department of Mining Engineering
VNIT, Nagpur
Date:

Department of Mining Engineering
Visvesvaraya National Institute of Technology, Nagpur

DISSERTATION APPROVAL SHEET

This dissertation entitled **"Analysing the Effect of Stoping Parameters on Stability of Decline: Malanjkhand Copper Project, HCL"** by **Mr. Gadamalla Rahul** is approved for the degree of **Master of Technology in Excavation Engineering.**

Dr. Sumant Mohanto	**Dr. Nikhil Ninad Sirdesai**	**Name:**
(Supervisor)	**(Co-Supervisor)**	**(External examiner)**
Name:		**Name:**
(Chairman)		**(Internal Examiner)**

Date:
Place: Nagpur

Department of Mining Engineering
Visvesvaraya National Institute of Technology
Nagpur

Non-Plagiarism Certificate

Certified that MTech. Dissertation titled **"Analysing the Effect of Stoping Parameters on Stability of Decline: Malanjkhand Copper Project, HCL"** submitted by **Gadamalla Rahul**, Enrollment No. **MT23EXV001** ID No. **30073** is original in nature and not copied from any literature material. Due credit has been given to the original researcher wherever referred.

MT23EXV001_GADAMALLA RAHUL

ORIGINALITY REPORT

19%	7%	11%	1%
SIMILARITY INDEX	INTERNET SOURCES	PUBLICATIONS	STUDENT PAPERS

Signature:
Name of the student: **Gadamalla Rahul**
Enrolment No: MT23EXV001
ID No. 30073

Signature:
Name of the supervisor: **Dr. Sumant Mohanto**
Assistant Professor, Department of Mining Engineering
VNIT Nagpur

Signature:
Name of the supervisor: **Dr. Nikhil N. Sirdesai**
Assistant Professor, Department of Mining Engineering
VNIT Nagpur

Acknowledgment

I would like to express my deepest gratitude to my supervisor, **Dr. Sumant Mohanto** and **Dr. Nikhil Ninad Sirdesai**, for their invaluable guidance, unwavering support, and constructive feedback throughout the course of this research. Your patience in guiding me through moments of uncertainty, your passion for knowledge, and your commitment to excellence have been nothing short of extraordinary. For all the hours you've invested, and the standards you've helped me rise to — I am, and always will be, profoundly grateful. Their expertise and encouragement have played a vital role in shaping this thesis from conception to completion.

I am also thankful to the faculty and staff of the **Department of Mining Engineering**, VNIT Nagpur, for providing the necessary resources, facilities, and a supportive academic environment. My sincere thanks to **Dr. Ajay Kumar Agarwal**, Head of the Department of Mining Engineering, VNIT Nagpur.

Special thanks to **Mr. Pramod Kubade** for his assistance during numerical model development and simulation in ANSYS Workbench.

I am profoundly grateful to **Shri Nagesh Shenoy sir** for providing essential data and technical insights during data collection from Malanjkhand Copper Project, HCL, which significantly enriched the scope of this work.

I would like to express my deepest appreciation and thanks to my batchmates and friends especially **Mr. Harshal Thakare, Mr. Sai Prakash, and Mr. Ajay Kumar** for emotional support, and help in this work.

Name: Gadamalla Rahul
Enrollment ID: MT23EXV001
Email ID: rahulgadamalla1016@gmail.com

Abstract

The present study focuses on three-dimensional finite element analyses of an underground hard rock mine operating below an exhaust open pit mine to determine the stability of decline considering *ANSYS Workbench Version 2023*. The case study mine considered for this study is Malanjkhand copper mine, which is located in the Balaghat district of Madhya Pradesh, India. The material constitutive model is considered to be elastoplastic in nature. The parameters considered for this study include sequence of extraction, distance between decline and stope boundary location on the footwall side, and variation in stope dimensions. The stability of D-shaped decline of cross-section dimension 5.5 m × 5 m has been studied considering the variation in parameters mentioned above. Two variations of stoping sequence are considered i.e., extraction of primary stopes from center towards extreme end, and primary stope extraction from extreme end towards the center along with worst case scenario where all the stopes are being extracted. Three variations of the distance between decline and stope boundary on the footwall side are considered, i.e., 150 m, 125 m, and 100 m away from stopes. In addition, three variations with stope dimensions are considered which include 20 m (W) × 41 m (H), 30 m (W) × 41 m (H), and 20 m (W) × 60 m (H) of stopes for the assessment of stability of decline, where W and H denotes width and height of the stopes, respectively. The results of the simulation models are assessed in terms of factor of safety and stress concentration factor. Based on the results obtained from the numerical simulation, it is observed that the sequence of extraction has no significant effect on the decline stability considering the existing geo-mining conditions. However, distance between decline and stope location plays a crucial role in determining the design of decline and its stability. The stope dimension also affects the stability of decline in conjunction with sequence of extraction considered for the present study.

Keywords: Decline stability, D-shaped opening, Factor of safety, Stress concentration factor, Finite element method

List of Figures

Figure No.	Title	Page No.
4.1	Google map of Malanjkhand mine (dated 10th May, 2025)	24
4.2	Dimension of trough and crosscut (All the dimensions are in m)	25
4.3	Dimension of (D-shaped) decline (Malanjkhand Copper Mine)	25
4.4	Three-dimensional numerical model considered for the present study	26
4.5	Orebody showing the stopes, decline and footwall drive	26
4.6	Pre-defined path A considered for mesh convergence study	27
4.7	Vertical displacement plot for different mesh sizes	28
4.8	Loading and boundary conditions considered for the numerical model	30
4.9	Schematic sketch of cases A1-A4 (Stope Extraction: from centre towards extreme end) and case C1 (All stopes extracted)	32
4.10	Schematic sketch of cases B1-B5 (Stope Extraction: Extreme end towards centre)	33
4.11	Case D1: Average distance of decline from production stopes: 150 m	34
4.12	Case D2: Average distance of decline from production stopes: 125 m	34
4.13	Case D3: Average distance of decline from production stopes: 100 m	34
4.14	Case E1: E1: 20 m (W) × 41 m (H)	35
4.15	Case E2: E1: 30 m (W) × 41 m (H)	35
4.16	Case E2: E1: 20 m (W) × 60 m (H)	35
4.17	Predefined paths considered for the numerical model	36
5.1	Factor of safety plots (A1-A4, C1) along path 1	38
5.2	Factor of safety plots (A1-A4, C1) along path 2	38
5.3	Factor of safety plots (A1-A4, C1) along path 3	39
5.4	Factor of safety plots (A1-A4, C1) along path 4	39

5.5	Factor of safety plots (B1-B5) along path 1	40
5.6	Factor of safety plots (B1-B5) along path 2	40
5.7	Factor of safety plots (B1-B5) along path 3	40
5.8	Factor of safety plots (B1-B5) along path 4	41
5.9	Maximum principal stress concentration factor plots along path 1	41
5.10	Maximum principal stress concentration factor plots along path 2	42
5.11	Maximum principal stress concentration factor plots along path 3	42
5.12	Maximum principal stress concentration factor plots along path 4	42
5.13	Minimum principal stress concentration factor plots along path 1	43
5.14	Minimum principal stress concentration factor plots along path 2	43
5.15	Minimum principal stress concentration factor plots along path 3	43
5.16	Minimum principal stress concentration factor plots along path 4	44
5.17	Factor of safety plots along path 1 for Case A1	44
5.18	Factor of safety plots along path 4 for Case A4	45
5.19	Factor of safety plots along path 1 for Case B5	45
5.20	Factor of safety plots along path 1 for Case B5	45

List of Tables

Table No.	Title	Page No.
4.1	Total number of elements for different mesh sizes	27
4.2	Material properties considered for the present study	29
4.3	Different cases analyzed for the study	31
5.1	FoS values for Cases A1, A4 and C1 for path 3	46
5.2	FoS values for Cases A1, A5 and C1 for path 4	46
5.3	FoS values for Cases B1 and B5 for path 1	46
5.4	FoS values for Cases B1 and B5 for path 2	47
5.5	FoS values for Cases A1, A4 and C1 for path 4	48
5.6	FoS values for Cases B1 and B5 for path 1	48

INDEX

	Chapter 1: Introduction	Page No
1.1	General	1
1.2	Background	1
1.3	Importance of the study	4
1.4	Objectives of the thesis	5
1.5	Scope of the thesis	5
1.6	Organisation of the thesis	6
1.7	Closure	6
	Chapter 2: Literature Review	
2.1	General	8
2.2	Stability assessment of underground structures in hard rock mines	8
2.2.1	Analytical methods	9
2.2.2	Empirical methods	9
2.2.3	Numerical modeling procedures	10
2.3	Design of decline for underground mine	12
2.4	Factors affecting stability of underground structures	12
2.5	Closure	14
	Chapter 3: Finite Element Method and Overview of Ansys Workbench Software	
3.1	General	15
3.2	Finite Element Method	15
3.3	ANSYS Workbench	16
3.4	Basics of ANSYS Workbench	16
3.5	Components of ANSYS Workbench	19
3.6	Closure	22
	Chapter 4: Development of three-dimensional Underground Mine Model	
4.1	General	23
4.2	Details of the mine site	23
4.3	Development of the numerical mine model	24
4.4	Mesh model and determination of suitable mesh size	26
4.5	Material properties considered for the numerical model	28
4.6	Pre-excavation stresses and boundary conditions	28
4.7	Different cases analyzed for the present study	30
4.8	Pre-defined paths considered for the numerical analyses	35
4.9	Closure	36
	Chapter 5: Results and Discussions	

5.1	General	37
5.2	Results of the numerical simulation	37
5.2.1	Effect of sequence of extraction	37
5.2.2	Effect of distance of decline from primary stope location	44
5.2.3	Effect of change in stope dimension	47
5.6	Closure	49
	Chapter 6: Conclusions and Future Scope of Work	
6.1	General	50
6.2	Conclusions	50
6.3	Future scope of work	51
	References	52

Chapter 1: Introduction

1.1 General

In excavation engineering, the stability of underground excavations is crucial for both the safety of the workers and the long-term success of mining operations. Stress distribution in the surrounding rock mass plays a vital role in determining the overall stability of the excavation. When an underground mine opening is made in a rock mass, the natural state of stress is disturbed, causing stress redistribution in the surrounding material. This redistribution can result in stress concentrations that may lead to rock failure, excessive deformation, or the need for additional reinforcement (Zhao et al., 2023). Consequently, understanding how the shape of an opening influences stress distribution is a critical aspect of mining engineering.

Creating large void space/excavation (also called open stopes in metal mines) in the underground due to ore extraction leads to stress redistribution in the surrounding rock mass which may adversely affect the stability of underground structures as well as open-pit slopes. The natural pillars left in the underground mine, i.e. crown and rib pillar play a crucial role in stabilizing the huge openings due to ore extraction. Openings with different geometries—such as circular, D-shaped, rectangular, or irregular shapes—behave differently when subjected to external loads (Cai et al., 2023). For instance, circular and D-shaped openings are known to distribute stresses more evenly than non-circular shapes. This is because the curved geometry of circular openings tends to reduce stress concentrations, which helps in increasing the overall stability of the surrounding rock. On the other hand, irregularly shaped openings, such as those with sharp corners or edges, tend to generate more concentrated stress fields, which can lead to localized rock failure (Dashkovska, 2022). Thus, understanding these differences is essential for designing safer and more efficient underground structures. The dimension and shape of primary openings plays a crucial factor in regulating the stability of the structures which stays throughout the mine's life along with other parameters such as material properties, shape of opening and distance from the primary stopes (Svrkota et al., 2015).

1.2 Background

Underground hard rock mining refers to extracting minerals and ores from solid rock formations beneath the earth's surface. Underground hard rock mining evolved from small-

scale prospecting to large-scale industrial operations. It is typically employed for ore bodies that are large, thick, or located in challenging geological conditions. The mining methods and equipment used in large-scale underground mining are designed to maximize resource recovery, ensure safety, and improve efficiency, which is reflected in underground mining operations such as sublevel stoping, room and pillar mining, block caving, and cut-and-fill mining. In India mining methods such as sublevel stoping¸ cut and fill, and room and pillar are employed for deeper mineral deposits like copper, lead-zinc, and chromite. These methods require careful planning and management to mitigate risks associated with ground instability drainage, ventilation, transportation, power supply, etc.

To obtain mineral deposits, we must develop ways/openings to reach deposits for the mining process to be created. There are three types of openings such as primary, secondary, and tertiary openings to reach mineral deposits. Each type serves distinct purposes and is selected based on factors such as the depth of the deposit, geological conditions, and economic considerations. Understanding these types of openings is crucial for efficient mine planning and operation. Primary openings are the initial access points to a mineral deposit and are critical for establishing the infrastructure needed for mining operations. They should be well maintained and kept stable through the mine life they should be maintained throughout the mine life.

- **Adits**: These are horizontal or nearly horizontal passages driven into the side of a hill or mountain. They are economical for accessing deposits located above the valley floor and are particularly suitable for hilly or mountainous terrains
- **Declines or Ramps**: These are inclined tunnels that provide access to shallow deposits. They are developed at a gradient of approximately 12% and allow for the transportation of materials and personnel using vehicles. Declines are increasingly popular due to their flexibility and lower initial costs compared to shafts
- **Vertical Shafts**: These are vertical tunnels used to access deep deposits, typically more than 300 meters below the surface. Although costly and time-consuming to construct, vertical shafts are preferred for their efficiency in transporting large volumes of ore and waste
- **Incline**: These are similar to vertical shafts but are developed at an angle. They are suitable for relatively shallow deposits and are less expensive than vertical shafts but require longer development lengths

Secondary openings are developed to facilitate the extraction of ore and include various types of tunnels and drifts. They should be well-maintained and kept stable throughout the planning period

- **Drifts**: These are horizontal passages driven along the ore body. They provide access to the ore and are used for transportation and ventilation
- **Crosscuts**: These are horizontal tunnels that connect drifts and are used to access different parts of the ore body. They also play a role in ventilation and material transport
- **Raise and winze**: These methods involve creating vertical or inclined openings to connect different levels of the mine. They are essential for ore extraction and ventilation

Tertiary Openings

Tertiary openings are used for specific functions such as ventilation, drainage, and additional access. They should be well-maintained and kept stable throughout the planning period.

- **Ventilation Shafts**: These are dedicated to ensuring adequate airflow throughout the mine, crucial for maintaining safe working conditions
- **Service Tunnels**: These are used for utilities such as water, electricity, and communication lines, supporting the overall operation of the mine
- **Escape Routes**: These are critical for safety, providing alternative exits in case of emergencies

The design and development of these openings must consider various factors, including geological stability, potential environmental impacts, and operational efficiency. Proper management of these aspects is essential to ensure the safety and productivity of underground mining operations to avoid or cause any accidents. The stability of an opening primarily depends on its ability to manage stress distribution effectively. Properly designed cross-sections can enhance the opening's stability by ensuring that stress is evenly distributed, thereby minimizing the risk of failure or deformation under load. The cross-section of the opening is determined by several factors, including its intended utilization, operational costs, and the patterns of stress distribution that it will encounter

The most widely used cross-sections used for underground excavation openings considered in the civil and mining industry include circular, elliptical, ovoidal, square, rectangular, D-shaped, and horse-shoe-shaped openings. Among all the shapes, circular, elliptical, and ovoidal openings impart uniform stress distribution in the surrounding rock strata; however, they are

expensive and difficult to construct. The rectangular and square openings with sharp edges are easy to construct but impose high stress concentration around the corners which generally results in spalling of the roof. The D-shape and horseshoe shapes have also stress distribution because they have an arching effect and are not as difficult to construct compared to circular, elliptical, and ovoidal openings. The access to the mineral deposits in underground mines mainly comprises shafts, declines, inclines, adit, crosscuts, drives, and drifts. Among all these openings, decline plays a very important role in the haulage or transportation of motorized vehicles in underground metalliferous mines.

1.3 Importance of the study

Decline is one of the crucial entries in mining operations, it serving as a main access point to the underground mine workings from the surface. A decline can be a Primary/ Secondary/ Tertiary inclined opening, driven to connect levels, usually in a downward direction, and used for the haulage of motorized vehicles. The smallest cross-section of decline should fit the largest machinery. The gradient of decline ranges from 1 in 7 to 1 in 12. The design of declines must also account for factors such as the type of material being transported, the expected traffic volume, and the geological conditions encountered during excavation. Thus, ensuring the stability of the decline is important, as any failure can lead to significant operational disruptions and safety hazards.

The following are the purpose of tunnel in excavation industry:

1. To provide safe access to the mineral deposit
2. To safely transport men, material, and machinery.
3. To provide ventilation.
4. It can be used as an emergency escape route

Mining in hard rock conditions has numerous challenges, especially when it comes to stabilizing structures such as declines over a long time. The excavation process can alter the stress distribution in the surrounding rock, leading to potential instability. This instability can result in displacement and deformation of decline, which pose significant risks to personnel and equipment. Hence it is important to analyse the effects of stress distribution on the decline during the excavation of stopes. Understanding the geotechnical properties of the surrounding rock mass is essential for maintaining the integrity of the decline and ensuring safe mining operations over time. Thus, it becomes pertinent to understand the stress distribution around

the decline with excavation of stopes, material properties, design of decline, and design of stopes to prevent failure in an underground structure and maintain operational efficiency.

1.4 Objectives of the thesis

The objectives of this thesis are as follows:

1. Development of three-dimensional finite element models considering Ansys *Workbench Version 23.0*
2. Analyzing the stability of decline with respect to the following parameters:
   A. Dimensional parameters of the decline including cross-sectional shape and depth
   B. Rock-mass Properties
   C. Stope design and stoping sequence
   D. Distance from the primary excavation zone

These objectives aim to provide a comprehensive understanding of surrounding rock mass behaviour subjected to the considered geo-mechanical conditions.

1.5 Scope of the thesis

Based on the above objectives, different tasks have been taken on to achieve each of the objectives of this thesis. A comprehensive literature review has been carried out for better understand of the effect of different parameters on the underground structures. The scope of work of this thesis are enumerated below-

1. Development of three-dimensional finite element models considering Ansys Workbench Version 23.0

Design of the LDBH stopes and pillars with primary and secondary openings involves the development of three-dimensional numerical models based on the finite element method using ANSYS *Workbench Version 23.0*. The three-dimensional models have been developed based on AUTOCAD files obtained from the case study mine. The simulation model consists of the underground mine model below the open pit mine with primary, secondary and tertiary openings including cross-cuts, extraction cross-cuts, footwall drive and hang wall drive. The laboratory data taken from the geotechnical report of the case study mine has been used as input for the numerical models. The insitu stress data obtained from the National Geophysical Research Institute (NGRI) have been incorporated in the numerical model.

2. Analyzing the stability of decline with respect to the following parameters:

Parametric study has been carried out to analyze the stability of decline considering variation in dimensional parameters of the decline including cross-sectional shape and depth, rock-mass properties, stope design and stoping sequence and distance from the primary excavation zone. The results of the numerical simulations have been assessed in terms of factor of safety, maximum and minimum principal stress concentration factor and equivalent plastic strain. Based on the obtained results, some useful conclusions have been inferred for the stability of decline under the considered variation in parameters.

1.6 Organisation of the thesis

This thesis is organized into the following chapters:

- Chapter 1 provides a general introduction, outlining the importance, objectives, and scope of the study.
- Chapter 2 presents a detailed literature review covering the importance of this research work.
- Chapter 3 presents a detailed description of the finite element method considered for the present study.
- Chapter 4 describes the detailed description of three-dimensional numerical modelling to determine the stability of decline in underground below an open-pit mine.
- Chapter 5 discusses the results obtained from the numerical models, highlighting the influence of key variables on stress distribution around the decline considering variation in different parameters.
- Chapter 6 presents the conclusions drawn from the study and offers recommendations for future work and practical application.

1.7 Closure

The introductory chapter has laid the groundwork for understanding the importance of stability of underground structures due to excavation activity. It has outlined the general background of the factors affecting stress distribution around openings and the growing importance of numerical modelling in geo-mechanical analysis. The objectives and scope of this thesis have been clearly defined, emphasizing the development of a representative numerical model and a parametric study focusing on dimensional parameters of the decline including cross-sectional shape and depth, rock-mass properties, stope design and stoping sequence and distance from

the primary excavation zone. These components collectively aim to provide a deeper understanding of the mechanical behavior of important parameters on surrounding rock mass.

In the following chapter, a comprehensive review of existing literature will be presented to examine the analytical and numerical methods for analyzing the stability of surrounding rock mass subjected to excavation.

Chapter 2: Literature Review

2.1 General

In excavation operations, accurately predicting the stress distribution around openings is crucial for effective excavation design and risk management. Stress concentration factors, which are influenced by the geometry of the opening, determine whether the surrounding rock will experience failure or excessive deformation. Areas with high stress concentrations may be prone to rock bursts, excessive ground movement, or tunnel collapses, all of which can jeopardize the safety of the excavation and increase operational costs (Cai et al., 2004). By understanding the impact of opening shape on stress distribution, engineers can design excavations that minimize these risks and ensure safer and more cost-effective mining operations. The present chapter deals with some of the widely accepted analytical methods and their limitation. The advantages of the numerical methods and literature related to stress distribution around excavation openings are also discussed in detail in this chapter.

The stability of underground mining openings is significantly influenced by both rock mass characteristics and stoping parameters. Since decline is one of the crucial entries in mining operations, serving as the main access point to the mining panel from the surface. Understanding these effects is crucial for ensuring the safety and efficiency of mining operations. The research papers provided offer insights into various methodologies and factors that affect the stability of declines, including rock mass variability, and geometry of decline and stopes. Hence designing a decline should be done effectively considering all the factors affecting a decline to remain stable throughout its service life to prevent production delays, loss of reserves, equipment damage, and injuries. There are hardly any studies conducted on the stability of declines. Therefore, developments such as haulage drives, footwall drives, and hanging wall drives are also taken into account because these developments experience similar conditions as the decline.

2.2 Stability assessment of underground structures in hard rock mines

Underground hard rock mining invariably involves the extraction of ore (stopes), leaving a portion of the ore in the form of natural pillars, i.e. crown and rib pillars. Stability of those pillars is an essential pre-requisite for maintaining safe working conditions in hard rock mines. The major factors governing the stability of pillars in underground metal mines include rock

mass properties, size of excavation, depth of working, orebody orientation, pre-existing in-situ stresses, backfilling and artificial support system (Herget 1988; Kvapil and Blake 1973; Tavakoli 1994; MOSHAB 1997; Edelbro 2003; Lu et al. 2009; Gabriel et al. 2011; Deb and Das 2011; Esterhuizen and Iannacchione 2011). Optimizing pillar dimension is one of the important concerns in metalliferous mines (Bakhtavar et al. 2010). Thick pillars left intact between two adjacent stopes (rib pillar), or between two levels (crown pillar) may provide additional support to the adjacent open stopes and hanging wall, with aid in the overall stability of the underground structures. However, it may be considered uneconomical from the mineral conservation point of view. At the same time, reducing the size of pillars results in instability issues, which may lead to roof collapse if one or more pillars fail (Mortazavi et al. 2009). Very few studies have been carried out so far to establish a design methodology and provide guidelines for pillar design (Betournay 1987; Betournay 1989; Hoek 1989). In general, assessment of pillar stability in metalliferous mines is carried out by either of the three methods, namely: (i) analytical methods, (ii) empirical methods and (iii) numerical modelling procedures.

2.2.1 Analytical methods

The analytical approach assumes mine roof as a beam or plate with the load applied over the beam, including the load of the overlying strata. In shallow mines, roof beam is assumed to be simply supported; whereas, for deep mines, it is considered to be with fixed ends. Overt and Duvall (1967) suggested formulas for calculating the maximum deflection, shear and tensile stresses on a simply supported uniformly loaded beam. However, designing open stopes considering analytical approach only caters to simple geometries (Kirsch 1898; Evans 1941; Adler and Sun 1968; Wright 1972; Ladanyi 1974; Brady 1977; Beer and Meek 1982; Brady and Lorig 1988); and hence, may not provide adequate solutions when dealt with complex geo-mining conditions.

2.2.2 Empirical methods

Most of the underground mines throughout the world still follow ‘rule of thumb’ or empirical methods for designing the open stopes and pillars to maintain the overall stability of the mine. A number of empirical design methods have been proposed by various researchers for pillar design and pillar strength determination (Salamon and Munro 1967; Bieniawski and van Heerden 1975; Hustrulid 1976; Mark and Barton 1997; York 1998; Brady and Brown 2003; Mark 2006; Mitri 2007; Jawed et al. 2013). Hedley and Grant (1972) analyzed the stability of

28 rib pillars (23 stable pillars, 2 partially failed and 3 crushed) in massive quartzites and conglomerates in an underground uranium mine. Based on the study, they proposed a formula to determine the pillar strength in hard rock condition. Later, in the subsequent years, several studies were then carried out for determining the empirical strength formula for hard rock pillars (Von et al. 1984; Krauland and Soder 1987; Hudyma 1988; Potvin et al. 1989; Sjoberg 1992; Lunder 1994; Lunder and Pakalnis 1997; Maybee 1999). Amongst the different empirical approaches, stability graph method is the most widely used and accepted method applied for open stope design; and is based on past data and rock mass classification systems. Since the stability zone depends on pre-existing historical mine data, the stability graph method is not suitable for designing open stope for mines which has no previous data. Over the years, the modifications have been implemented by different researchers to cater to the shortcomings of the stability graph method (Laubscher 1977; Mathews et al. 1980; Diering and Laubscher 1987; Potvin and Milne 1992; Stewart and Forsyth 1993; Hadjigeorgiou et al. 1995; Suorineni et al. 1999; Trueman et al. 2000; Mawdesley et al. 2001; Bewick and Kaiser 2009; Mitri et al. 2011). However, there hardly exists any literature related to determine the stability of D-shaped decline in underground metalliferrous mines.

2.2.3 Numerical modeling procedures

Analytical and empirical approaches do not thoroughly analyze the behaviour of the surrounding rock medium around the excavated profiles in the underground. In this context, numerical methods prove to be the only viable option to cater to the ground control issues in mining because of their strong theoretical foundation, potential to scale up and visualization capabilities. Numerical methods solve the shortcomings of the above methods of designing open stopes and pillars as it easily compensates complex geometries incorporating failure criteria to assess the effect of induced stresses around the underground openings. In recent years, three-dimensional numerical methods have gained wider acceptance in geo-mining stability issues such as mine design and feasibility studies.

A lot of research has been carried out over the years to cater to the stability issues of underground structures in metalliferous mines under various geo-mining conditions. Stability of sublevel open stopes using non-linear two-dimensional finite element analysis was studied by Chen et al. (1983) at a depth of 1200 m, considering parameters such as stope height, stope span, rib pillar width and the number of open stopes. Martin et al. (1999) studied the stability of stope hanging wall with two-dimensional finite element models considering the effect of low confinement around the open stopes. Zhang and Mitri (2008) studied the stability of a

haulage drift due to surrounding mining activities with two-dimensional non-linear elastoplastic finite element models. The mining method employed for extracting the ore was sublevel stoping with delayed backfill. A detailed parametric study was carried out considering factors such as rock mass properties, mining depth and distance from the orebody extraction. A two-dimensional numerical study was conducted to study the pillar behaviour in deep underground mine under high-stress conditions (Mortazavi et al. 2009). The study inferred that at high width-to-height ratios, the pillar behaves in elastic range in a very stiff manner indicating a high load-bearing capacity. However, at low width-to-height ratios, the load-bearing capacity drops, resulting in pillar failure. Wang et al. (2013) carried out three-dimensional finite element analysis to study the stability issues of backfilling in a subsiding area. It was found that optimizing the stoping sequence resulted in minimizing the stress concentration around the stope; thereby, ensuring safety in stope extraction. Trinh and Jonsson (2013) proposed the design consideration of an underground room in a hard rock mine subjected to high horizontal stresses with sublevel caving as the method of ore extraction. The results obtained from the numerical simulation agreed well with the experiences encountered during construction of the underground room such as overbreak observed in the roof, shotcrete cracks in the roof, shorter bolts used in the sidewalls and longer bolts in the roof. Abdellah et al. (2014) simulated three-dimensional numerical analyses to study the stability of mine development intersections at different levels of an underground mine. The study showed that there is a lateral shift in development intersection, with high shear stress accumulation in the roof. Kumar et al. (2017) analyzed a steeply dipping orebody with width reduction as the depth of working increases. Two-dimensional finite element analyses were carried out using ANSYS software, considering Drucker-Prager yield criterion. A multi-variate regression model was developed for determining the safety factor of crown pillars based on the parametric study carried out varying the parameters including rock properties such as geological strength index (*GSI*), uniaxial compressive strength (UCS), Young's modulus (*E*) and thickness of the crown pillar. Naung et al. (2018) carried out three-dimensional numerical simulations to study the stability assessment of open stopes under overlaying mined-out regions. A parametric study was carried out for given geo-mining condition varying parameters such as barrier pillar height, stope width, stress ratio, geological condition and backfill material. The other important literatures related to numerical modelling in underground mines considering quasi-static loading condition include Pariseau (1980), Wold (1980), Sinclair et al. (1981), Baria (1984), Mitri et al. (1995), Martin and Maybee (2000), Aubertin et al. (2003), Ferrero et al. (2010), Gonen and Kose (2011), Idris et al. (2011), Wang et al. (2012), Li et al. (2013) Purwanto et al.

(2013), Kushwaha et al. (2014), Yang et al. (2015), Himanshu et al. (2017), Liu et al. (2018) and Shnorhokian et al. (2018). However, there is hardly any literature related to the stability of decline in an underground hard rock mine operating below a surface mine.

2.3 Design of decline for underground mine

The purpose of designing a mine decline is to develop a more effective layout that minimizes both the costs of development and transportation over the mine's operational period. The selection of the decline's cross-section must be done with great care to guarantee optimal space usage and efficient stress distribution. An increased span length can lead to greater instabilities, and the choice of cross-section contributes to effective stress management. Any shape featuring corners tends to exhibit higher stress concentrations at those edges, which is why blended shapes like horse-shoe, D-shaped, and rectangular or square forms with rounded corners are preferred for enhanced stress distribution to reduce failure risks.

Optimizing the arrangement of access galleries can be viewed similarly as addressing a network flow challenge, focusing on shortening excavation lengths and cutting down transportation distances. Dubin's paths serve as a foundational framework for crafting efficient designs by enhancing both the geometric characteristics and operational constraints of the decline. The Decline Optimisation Tool (DOT) is capable of simulating various decline configurations, allowing for a comprehensive evaluation of potential designs tailored to different operational contexts. By integrating geotechnical information and operational parameters, DOT formulates optimized decline pathways that lower costs while enhancing safety and efficiency within underground mining operations.

2.4 Factors affecting stability of underground structures

Rock mass properties

Factors such as the type of rock, its strength, and deformation characteristics must be carefully assessed to guarantee that the decline can endure the stresses exerted during excavation and operational activities. Gaining insight into these attributes facilitates the design of safe and effective mining openings that comply with operational needs and geological settings. Based on the Geological Strength Index (GSI), rock masses are examined to evaluate the stability of the decline, indicating that a poorer rock mass leads to a broader yield zone, which signifies a larger area vulnerable to failure, whereas a good rock mass tends to remain stable. This implies that mines operating under weaker rock conditions require additional protective measures. The

design of the decline necessitates a comprehensive understanding of geological conditions; overlooking this aspect can result in heightened deformation or failure in the adjacent rock layers over time, prompting the need for rehabilitation efforts. Understanding how differences in rock mass quality, shown by systems like the Geological Strength Index (GSI), Rock Mass Rating (RMR), and Q-System, can help in the safety of mining process.

Stope design parameters

Stope design plays a vital role in underground mining, as it significantly influences ore recovery and the integrity of surrounding rock. A successful stope design must take into account aspects such as ore shape, rock mass characteristics, and the order of excavation to reduce dilution and enhance resource extraction while prioritizing safety throughout the mining operation. The stability of individual openings and subsequently broaden the discussion to include the possible overlap of failure zones among adjacent excavations. This helps in understanding the correlation between neighbouring excavations and individual openings which are frequently underestimated in conventional methods, while employing techniques like transverse and longitudinal stoping with delayed backfill face challenges in maintaining safe and stable mine openings. These methods influence the extent of mine development needed, as well as the stability of haulage drifts and junctions.

Stoping sequence

The stress induced by mining exhibits considerable variation throughout the progression of the mining activities. This means that, at the start, the intersection is more than safe enough compared to how much stress is being imposed by the mining process. However, as additional stopes are mined from different levels and found that the safety factor diminishes. The research also emphasizes the effects of same-level mining exert a more significant negative effect on its stability compared to mining at a lower level. The numerical model indicated that the lateral displacement is more prominent when stopes are mined at the same level, particularly resulting in higher lateral displacements. During the mining operation, a specific rock formation referred to as "squeezing-type" was discovered which causes high deformation of the rock mass. This necessitated considerable rehabilitation efforts to guarantee safe access to the ore.

Distance from the primary excavation zone

Understanding the distance from the primary excavation zone is critical for evaluating the stability of declines and other underground openings, as it directly influences stress distribution

and potential ground failure. The nearer the excavation is to the orebody, the higher the likelihood of yielding or breakage in the adjacent rock, a phenomenon that has been documented. Variables such as mining depth, the gap between the stope and haulage drift, and the sequential extraction of ore blocks are essential for comprehending stress redistribution patterns and creating yield zones around drifts.

Underground mine support system

The underground mine support system plays a crucial role in ensuring the safety and stability of mining operations beneath the Earth's surface. As mining activities extend deeper into the ground, the challenges associated with ground control and structural integrity become increasingly complex. These support systems are designed to withstand the immense pressures and dynamic forces encountered in subterranean environments, thereby preventing collapses and protecting the workforce. The study highlights the importance of understanding the geological conditions when designing support systems in mining. The unexpected deformations were largely due to the weak rock formations, which were not fully accounted for in the initial models.

2.5 Closure

The present chapter focused on the literature related to stability of pillars and openings in underground metalliferrous mines considering analytical, empirical and numerical methods. Further, the importance of numerical methods over other methods is discussed with few important literatures on distribution of stresses around excavation openings.

Chapter 3: Finite Element Method and Overview of Ansys Workbench Software

3.1 General

The stress distribution around excavations is a critical aspect of geotechnical engineering, particularly when utilizing Finite Element Method (FEM) analyses. Various studies have demonstrated how excavation techniques influence stress states and ground displacements, revealing significant insights into the behavior of surrounding materials. Excavating an opening in the ground, whether for tunnels, mines, or underground structures, disrupts the existing state of stress in the surrounding rock or soil mass. This disruption leads to a redistribution of stresses, resulting in concentrated stress zones around the opening. Understanding and predicting these stress changes are paramount in geotechnical engineering to ensure the stability and safety of the excavation and any nearby structures.

Before excavation, the ground is in a state of in-situ stress, which comprises vertical stress due to the weight of the overlying material and horizontal stresses that are influenced by geological history, tectonic activity, and depth. The magnitudes and orientations of these principal stresses vary significantly with location and depth. Upon excavation, the material that was supporting the in-situ stresses is removed, causing the surrounding mass to carry the load. This leads to a concentration of stresses around the perimeter of the opening.

For calculating these stresses, the underground openings are analysed using closed form solution and numerical methods (FEM in this case). In this chapter, the Finite Element Method formulation, its application to thermo-mechanical analysis of underground storage system and a brief introduction to ANSYS has been dealt with.

3.2 Finite Element Method

The Finite Element Method (FEM) is a powerful numerical technique used to find approximate solutions to a wide range of engineering and mathematical physics problems. It's particularly valuable for problems with complex geometries, boundary conditions, or material properties where analytical solutions are difficult or impossible to obtain. The fundamental principle of FEM is to divide a complex problem domain into smaller, simpler parts called finite elements. These elements are interconnected at specific points called nodes. Instead of solving the governing equations over the entire complex domain, FEM solves simpler equations for each

individual element and then assembles these solutions to obtain an approximate solution for the whole system. The global system of equations is developed as follows:

$$\{F\} = [K]\{q\} \quad (3.1)$$

where,

{F}: global force vector, i.e., forces in each node,

[K]: global stiffness matrix based on material properties,

{q}: displacement vector containing each node.

The known boundary conditions of the problem (e.g., fixed displacements, applied forces, specified temperatures) are applied to the global system of equations. This step modifies the equations and reduces the number of unknowns. The resulting system of linear algebraic equations (or sometimes non-linear equations) is solved using appropriate numerical techniques to obtain the values of the primary variables at the nodes. The resulting system of linear algebraic equations (or sometimes non-linear equations) is solved using appropriate numerical techniques to obtain the values of the primary variables at the nodes.

3.3 ANSYS Workbench

Ansys Workbench is a capable finite element analysis (FEA) tool that can be used for a wide range of geotechnical engineering analyses, particularly for complex soil-structure interaction problems, rock engineering problems, static analyses, dynamic analyses, and coupled field problems. However, users need a good understanding of geotechnical principles and FEA techniques to effectively utilize it. For certain specialized geotechnical analyses or for users seeking a more tailored interface, dedicated geotechnical software or add-on.

3.4 Basics of ANSYS Workbench

Ansys Workbench is a powerful and user-friendly platform that integrates various Ansys simulation software tools into a single environment. It provides a project-based workflow that guides you through the different stages of an engineering simulation. Here are the basic concepts of Ansys Workbench:

1. Project Schematic:

- This is the central hub of Ansys Workbench. It visually represents the simulation process as a flow chart of interconnected **Analysis Systems**.

- Each **Analysis System** represents a specific type of simulation (e.g., Static Structural, Thermal, Fluid Flow) and consists of several linked cells that represent different stages of the analysis.
- The flow of data between these cells is indicated by arrows, showing the dependencies between different steps.

2. Analysis Systems:

- These are pre-defined templates for different types of engineering simulations.
- You can drag and drop various Analysis Systems from the **Toolbox** onto the Project Schematic.
- Common Analysis Systems include:
    - **Static Structural:** For analyzing stresses and deformations under static loads.
    - **Transient Structural:** For analyzing time-varying loads and dynamic effects.
    - **Thermal Analysis (Steady-State & Transient):** For analyzing heat transfer.
    - **Fluid Flow (Fluent or CFX):** For computational fluid dynamics simulations.
    - **Modal Analysis:** For determining natural frequencies and mode shapes of a structure.
    - **Harmonic Response:** For analyzing the response of a structure to sinusoidal loads.
    - **Explicit Dynamics:** For simulating high-speed, short-duration events like impacts.
    - **Electrostatics/Magnetostatics:** For electromagnetic field simulations.

3. Cells:

Each Analysis System is made up of several cells, representing the key steps in a simulation:

- **Geometry:** This cell is where you define or import the CAD geometry of your model. You can use Ansys SpaceClaim (a built-in 3D modeler) or connect to various CAD software packages.

- **Mesh:** Here, you discretize the geometry into a finite element mesh. You can control element size, type, and refinement to achieve the desired accuracy.
- **Setup:** In this cell, you define the physics of your problem, including material properties, boundary conditions (loads, supports, thermal conditions, etc.), and analysis settings.
- **Solution:** This cell contains the solver settings and is where you initiate the simulation.
- **Results:** After the solver finishes, this cell allows you to post-process the results, such as viewing stress contours, displacement plots, temperature distributions, and generating reports.
- **Parameters (Optional):** This cell allows you to define input and output parameters for design studies, optimization, or sensitivity analysis.

4. Toolbox:

- Located on the left side of the Workbench window, the Toolbox contains a library of available Analysis Systems and Components.
- You can browse by physics (e.g., Mechanical, Fluid Flow, Thermal, Electromagnetic) or by component type.
- Double-clicking or dragging an item from the Toolbox adds it to your Project Schematic.

5. Properties Window:

- Typically located on the right side, the Properties window displays the settings and options for the currently selected cell or object in the Project Schematic or within a specific cell editor (e.g., Mechanical).
- You can modify various parameters and settings in this window.

6. Menu Bar and Toolbar:

- The Menu Bar at the top provides access to various commands for file management, editing, viewing, and managing the project.
- Toolbars provide quick access to commonly used functions.

Basic Workflow in Ansys Workbench:

1. **Drag and Drop an Analysis System:** Choose the appropriate analysis type from the Toolbox and drag it onto the Project Schematic.
2. **Define Geometry:** Either import an existing CAD model or create a new one using Ansys SpaceClaim (accessed by double-clicking the Geometry cell).
3. **Mesh the Geometry:** Double-click the Mesh cell to open the Meshing editor. Generate a suitable finite element mesh for your geometry.
4. **Set Up the Physics:** Double-click the Setup cell to define material properties, boundary conditions, loads, and other relevant physics for your chosen analysis type.
5. **Solve the Model:** Double-click the Solution cell and define the desired results to be calculated. Then, initiate the solver.
6. **Review Results:** Double-click the Results cell to open the post-processing environment. Visualize and analyze the simulation results using various tools and plots.
7. **Save the Project:** Save your Ansys Workbench project to preserve your work. The project file (.wbpj) stores all the data and links to the individual analysis files.

Ansys Workbench's intuitive interface and integrated workflow make it a powerful tool for engineers to simulate and analyze complex engineering problems across various disciplines. Understanding these basic elements is the first step towards effectively using Ansys for your simulations.

3.5 Components of ANSYS Workbench

When **Static Structural** analysis system is dragged into the Project Schematic in Ansys Workbench, it comes with a set of interconnected cells that represent the different stages of the analysis. Here are the fundamental components (cells) and what they entail:

1. **Engineering Data:**
   - This cell defines the material properties that will be used for your simulation.
   - Double-clicking this cell opens the **Engineering Data Editor**.
   - Here, we can:

- Select materials from the Ansys material library (which includes common structural materials like steel, aluminum, etc.).
- Define new materials with specific properties (e.g., Young's Modulus, Poisson's Ratio, Density, Yield Strength, Tangent Modulus for plasticity, etc.).
- Edit the properties of existing materials.
- Create material models that account for temperature dependency or other complex behaviors.

- A green checkmark on this cell indicates that material properties have been defined.

2. **Geometry:**

- This cell is where you define or import the geometric model of the part or assembly you want to analyze.
- Double-clicking this cell opens the **Geometry Editor**. By default, Ansys Workbench uses **Ansys SpaceClaim** for direct modeling, but you can also link to other CAD software packages.
- In the Geometry Editor, you can:
  - Create a new geometry from scratch.
  - Import geometry files from various CAD formats (e.g., STEP, IGES, Parasolid, SolidWorks, CATIA).
  - Modify and prepare the geometry for meshing (e.g., surface repair, mid-surface extraction).
- A green checkmark on this cell indicates that a geometry has been defined.

3. **Model:**

- This is the core of the setup process where you define the finite element model.
- Double-clicking this cell opens **Ansys Mechanical**, a comprehensive FEA pre-processing, solving, and post-processing environment.
- Within Ansys Mechanical, you perform the following crucial steps:

- **Mesh Generation:** Discretize the geometry into a network of finite elements (e.g., tetrahedra, hexahedra). You control element size, shape, and refinement.
- **Coordinate Systems:** Define local or global coordinate systems as needed for applying loads, boundary conditions, or interpreting results.
- **Named Selections:** Create groups of geometric entities (faces, edges, vertices) or elements for easier application of loads, boundary conditions, and result scoping.
- **Contacts:** Define how different parts of an assembly interact with each other (e.g., bonded, frictional, no separation).
- **Boundary Conditions:** Apply constraints (fixed supports, displacements) to restrict the movement of the model.
- **Loads:** Apply forces, pressures, moments, torques, and other types of mechanical loads to the model.
- **Analysis Settings:** Configure the solver parameters, such as the number of steps, convergence criteria, and output controls.

o A green checkmark on this cell indicates that the model has been set up with a mesh, boundary conditions, and loads.

4. Solution:

o This cell defines the results you want to extract from the analysis.

o Double-clicking this cell in Ansys Mechanical allows you to insert various result items, such as:

- **Deformation:** Total deformation, directional deformation.
- **Stress:** Equivalent (von-Mises) stress, principal stresses, normal stress, shear stress.
- **Strain:** Equivalent strain, elastic strain, plastic strain.
- **Reaction Forces/Moments:** Forces and moments at the supports.
- **Contact Results:** Contact pressure, contact status, frictional stress.

- Once the setup in the "Model" cell is complete, you right-click on the "Solution" cell and choose "**Solve**" to run the simulation.
- A green checkmark on this cell indicates that the solver has successfully completed the analysis.

5. **Results:**
   - This cell allows you to visualize and analyze the results calculated in the "Solution" step.
   - Double-clicking this cell opens the post-processing environment within Ansys Mechanical.
   - Here, the following can be done:
     - View contour plots of stresses, strains, displacements, etc.
     - Create animations of the deformation.
     - Generate graphs and charts of results along specific paths or at specific locations.
     - Create reports summarizing the analysis and results.
     - Evaluate safety factors based on stress results.
   - A green checkmark on this cell indicates that the results have been reviewed.

These five main cells form the fundamental workflow for performing a static structural analysis in Ansys Workbench. By systematically working through each cell, you can define your problem, solve it using the finite element method, and interpret the results to gain insights into the structural behavior of your design.

3.6 Closure

In this chapter, the finite element analysis along with the different steps to it has been described. This is followed by a description of ANSYS *Workbench Version 2023* and its main features.

Chapter 4: Development of Three-Dimensional Underground Mine Model

4.1 General

In the present study, three-dimensional finite element models have been developed for Malanjkhand copper mine, which is a hard rock underground mine, operating below an open pit mine. The numerical models have been developed based on AUTOCAD files of plans and longitudinal sections obtained from the mine. The underground mine model consists of the open pit boundary along the primary and secondary openings such as decline, crosscuts, footwall drive, hang wall drive, extraction crosscut, drill crosscut and trough crosscut. A total of 46 finite element models are developed including 2 in-situ models (without any mining activity) to determine the stability of decline considering variation in different parameters. The different cases analyzed for the present study have been discussed in detail in this chapter.

4.2 Details of the mine site

The mine site considered for the study is Malanjkhand underground copper project, which is the largest copper deposit in India. The mine is located at a distance of 90 km away north-east to Balaghat district of Madhya Pradesh, India located at altitude of 575 mRL. The ore body found in Malanjkhand copper project falls under Shitalpani block. The quartz vein and mineralized granite is the main host of the mineral deposit. The major copper ore in the region comprises of chalcopyrite, alongside pyrite and magnetite. The ore body has a strike length of approximately 2200 m, average thickness varying between 65 -100 m. Hence, transverse method of stope extraction is adopted with large diameter blasthole (LDBH) stoping method. The average dip of the orebody is around 65° with a dyke intrusion in the central part of the deposit, along part of shear plane. Thus, the mine is divided into two broad parts, i.e., North and South mine (Mohanto and Deb, 2020). Figure 1 shows the google map of the Malanjkhand copper mine showing the open pit mine along with the location of the north and south decline.

The open pit mine has been exhausted since year 2022 as it has attained its ultimate pit bottom. The production from the underground mine for the first level has begun and development work is in progress for the 2nd and 3rd level, respectively. Large diameter blasthole (LDBH) tranverse stoping method is adopted for stope extraction as thickness of the orebody exceeds 20 m. In this method, large diameter holes of 165 mm will be drilled from the drill drive in a ring pattern

and will radiate outwards to the boundary of ore block being mined. Paste backfilling will be carried out to fill the void open stopes to provide confinement to the surrounding pillar walls. A solid surface barrier pillar of 40 m is left intact between the ultimate pit bottom (340 mRL) and first level stopes (300 mRL). The decline for the underground mine has reached till the bottom portion of the second level, which connects to the footwall drive and thereby providing access to the stopes at the first level. The stope height of 56 m is maintained for the first level stopes including the trough and two adjacent primary stopes are to be extracted to achieve the production target of the underground mine.

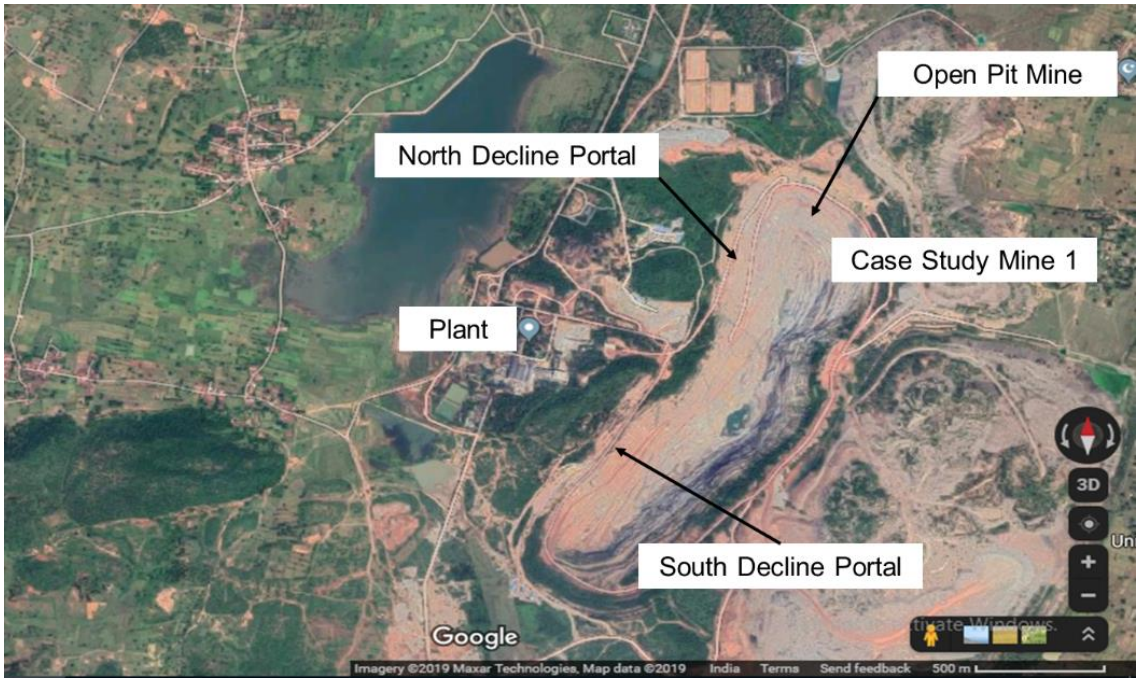

Figure 4.1 Google map image of Malanjkhand mine (dated 10th May, 2025)

Figure 4.2 shows the dimension of the trough and crosscut for the underground mine. The dimensions of these declines are selected as an extended D-shape section with a dimension of 5.5 m × 5.0 m, as shown in Figure 4.3. The portal of the North mine decline is located at 532 mRL on the footwall side as per the approved mining plan (IIT Kharagpur report, 2017).

4.3 Development of the numerical mine model

The three-dimensional numerical model considered for the study incorporates detail geological information like the orientation of the orebody, basic dyke, and other intrusions in the country rock, and are referred from the geological plans and sections provided by the mine. The actual mine dimensions of crosscuts, hanging wall, footwall, trough drive, drill drive, stope, barrier crown pillar and rib pillar are incorporated into the model. To avoid complexity and complication in 3D model, the geological sections are digitized using A*utoCAD* software

in a simplified form to represent the orientation of the orebody and country rock and then exported to ANSYS Workbench 23.0 for further simulation. Figure 4.4 shows the 3D underground mine model, located below the open-pit excavation with first level of working. The thickness of the ore body varies between 60 m and 75 m, and hence transverse stoping is adopted. The dimensions of crosscuts, trough crosscuts and drill crosscuts in the numerical model are considered as 4.5 m × 4.0 m. The base numerical model has been developed after mesh convergence is carried out. The outer dimension of the model is 2100 m (length) × 1750 m (breadth) × 750 m (height) (Figure 4.4). The numerical model consisting of orebody with stopes, decline and footwall drive is shown in Figure 4.5.

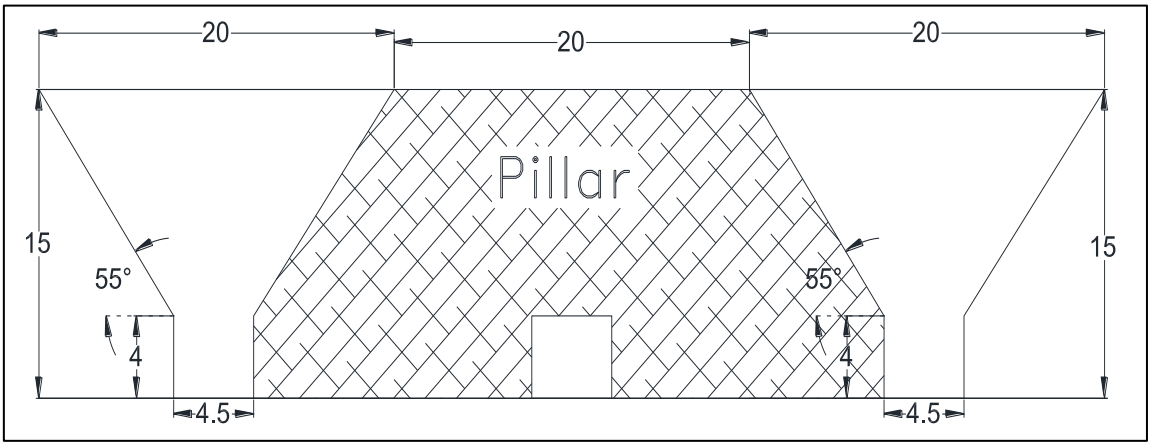

Figure 4.2 Dimension of trough and crosscut (All the dimensions are in m)

Figure 4.3 Dimension of (D-shaped) decline (Malanjkhand Copper Mine)

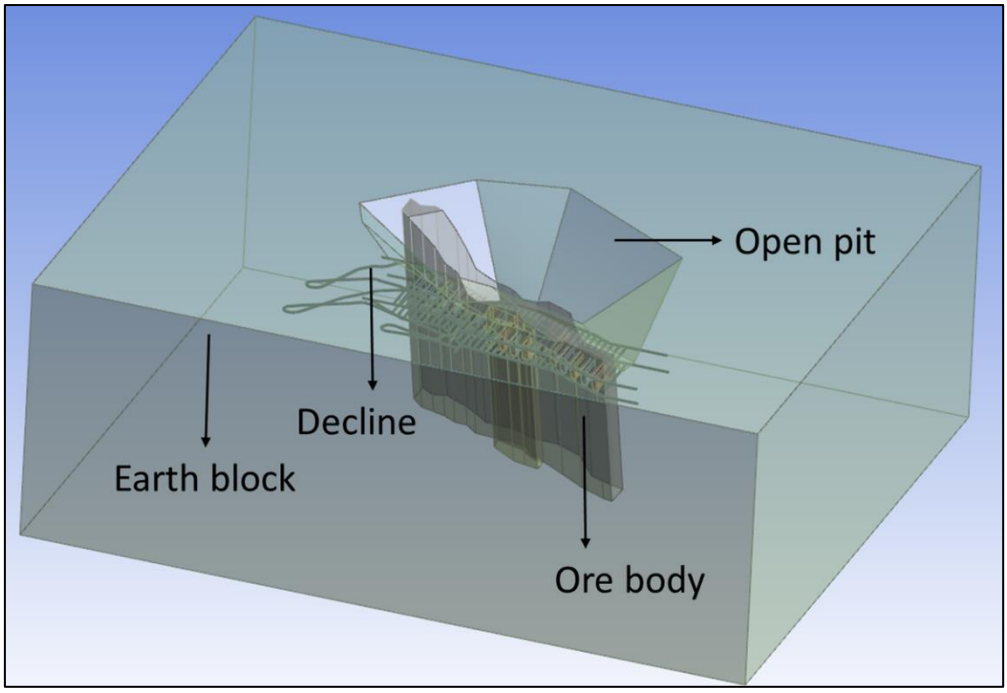

Figure 4.4 Three-dimensional numerical model considered for the present study

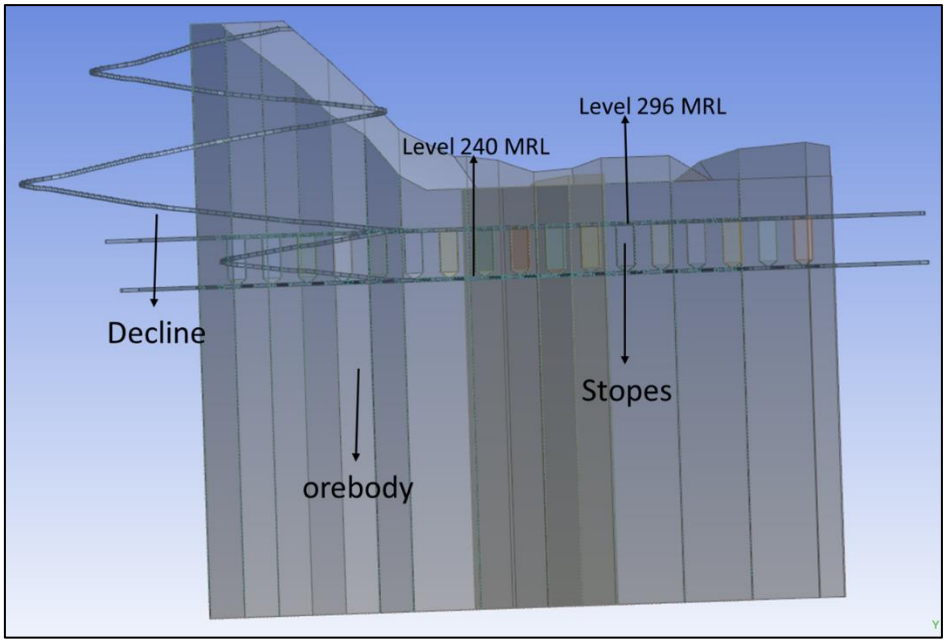

Figure 4.5 Orebody showing the stopes, decline and footwall drive

4.4 Mesh model and determination of suitable mesh size

Figures 4.6 shows the meshed model of the three-dimensional FEM model considered for the present study. Tetrahedron and hexahedral elements are used for meshing to fit the best source and target for the numerical model. Finer elements are used around the mined-out stopes and excavated profiles, which offer the advantage of accommodating high-stress gradients; whereas, coarser elements are used in the rest volumes to reduce the number of elements,

thereby minimizing the computational time. Mesh convergence study has been carried out to establish the mesh size of the reference model.

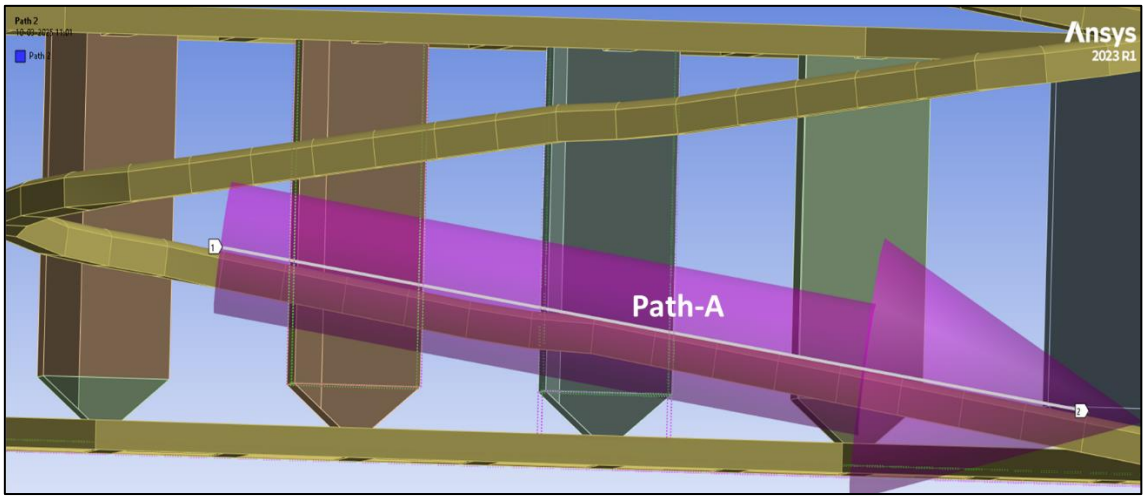

Figure 4.6 Pre-defined path A considered for mesh convergence study

In order to determine the mesh size, the base FEM model is analyzed considering 3 m, 4 m, 7.5 m and 10 m minimum element sizes. Table 4.1 shows the total number of elements generated for different mesh sizes. Figures 4.7 shows the vertical displacement plots for different element sizes along path A for reference model with first level extraction. The percentage change in average vertical displacement along path A for 4 m, 7.5 m and 10 m element size are found to be 2.2 %, 6.7% and 28.8 % as compared to 3 m element size. The results show that there exists no significant change for 3 m and 4 m element sizes; hence, to reduce the overall simulation time, the minimum size of the element is considered to be 4 m for the present analysis.

Table 4.1 Total number of elements for different mesh sizes

Sl.no	Element Size	No. of nodes	No. of elements
1	10 m	2173293	1567393
2	7.5 m	5191232	4707287
3	4 m	9229878	7262552
4	3 m	15730709	11467034

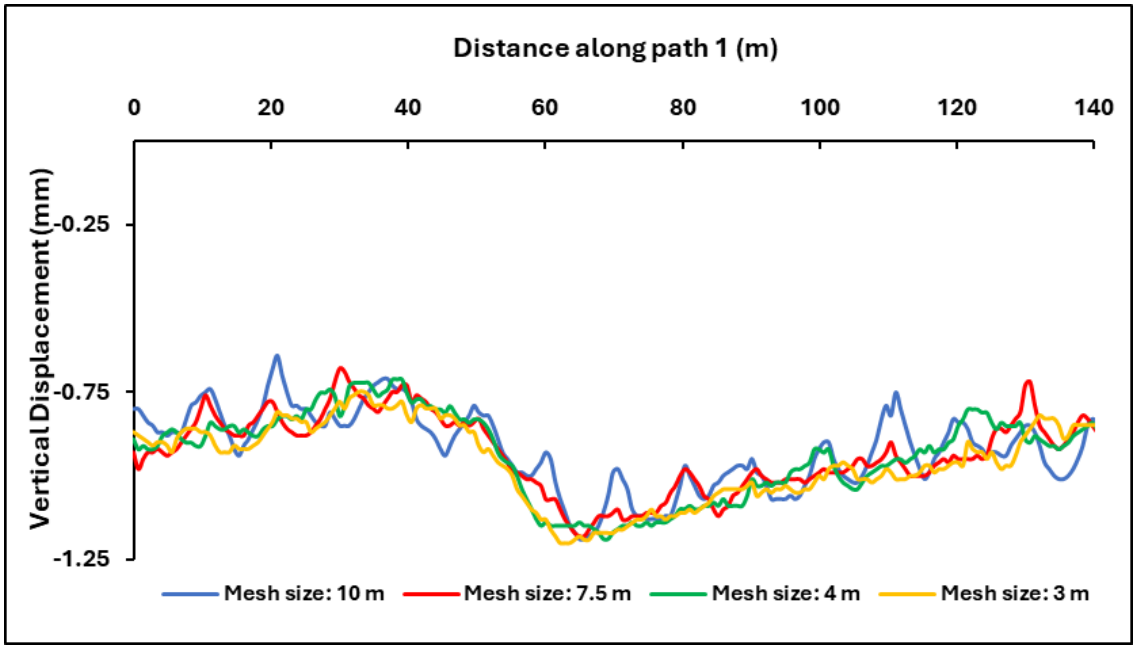

Figure 4.7 Vertical displacement plot for different mesh sizes

4.5 Material properties considered for the numerical model

RocData version 4.0 (RocData User's Manual Version 4.0) is used to reduce the intact rock properties to rock mass properties (equivalent rock mass modulus, rock mass strength, cohesion c and angle of internal friction ϕ by providing necessary input parameters such as uniaxial compressive strength σ_{ci} and elastic modulus of intact rock E_i, geological strength index *GSI*, intact rock parameter m_i and disturbance factor D (. Thus, for analysis of field conditions, the magnitudes of intact rock properties do not provide a realistic picture of those of rock mass. The material behaviour of rock is modelled as elastoplastic material having Drucker-Prager yield criterion. Table 4.2 show the rock mass properties for orebody (OB) and waste rock (WR) considered for the present study. σ_{cm}, E_m, ϕ_m, c_m, σ_{bm} and σ_{tm} refers to the uniaxial compressive strength of rock mass, modulus of elasticity of rock mass, internal friction angle of rock mass, cohesion strength of rock mass, biaxial compressive strength and tensile strength of the rock mass, respectively.

4.6 Pre-excavation stresses and boundary conditions

The major (σ_H) and the minor (σ_h) principal horizontal stresses are evaluated using equation (4.1) and (4.2) as provided by Geotechnical Investigation Report (1992):

$$\sigma_H = (6.3 + 0.033\,z)\ \text{MPa} \qquad (4.1)$$

$$\sigma_h = (5.7 + 0.061\ \mathrm{z})\ \mathrm{MPa} \quad (4.2)$$

where z = depth from the ground surface (m)

In-situ stresses are applied onto the model side faces in two perpendicular vertical faces; the opposite faces are constrained in x-direction and y-direction, respectively, as shown in Figure 4.5. The variation in-situ stresses is done based on depth from surface, having uniform increasing trend with depth. The σ_{Hmax}/σ_v and σ_{Hmin}/σ_v are considered to be 1.63 and 0.94, respectively as calculated using the above equations, where σ_v is the vertical stress. The bottom face is also constrained to restrict the movement in z-direction in the Cartesian coordinate system. Gravity loading is also applied as g = 9.81m/s^2 in the vertical downward direction.

Table 4.2 Rock mass properties considered for the present study

Material Properties	Particulars	
	Orebody	Waste Rock
GSI	65	65
D	0.5	0.3
σ_{cm} (MPa)	13.8	17.5
E_m (GPa)	8.5	11.1
ϕ_m (deg.)	54.7	56.4
c_m (MPa)	3.6	4.0
σ_{bm} (MPa)	14.8	18.6
σ_{tm} (MPa)	1.36	1.8

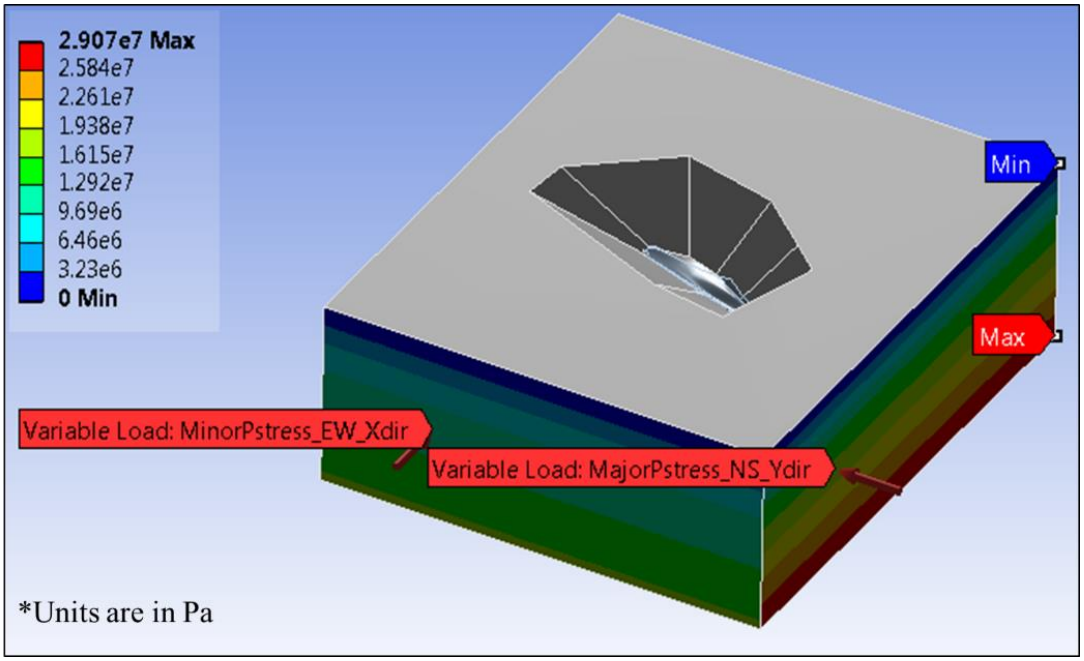

Figure 4.8 Loading and displacement boundary conditions

4.7 Different cases analyzed for the present study

The reference (base) numerical model considered for the study consists of the conditions prevailing in the field. To analyze the effect of various parameters on the stability of decline, parametric study has been carried out considering variation in sequence of extraction, distance of decline from the first level stope location and stope dimensions. Table 4.3 shows the brief description of the different cases analysed to study the effect on the decline located at around 150 m away from the stope location. A1-A4 include four cases with primary stopes being extracted from centre towards extreme end on either side with 2, 4, 6 and 8 stopes, respectively; whereas, B1-B5 include five cases with primary stopes being extracted from extreme end towards the centre with extraction of 2, 4, 6, 8 and 9 stopes, respectively. Case C1 depicts the worst scenario where all primary and secondary stopes of the first level are extracted. Figure 4.9 shows the schematic sketch of cases A1-A4 and C1 (worst scenario); whereas, figure 4.10 shows the schematic sketch of cases B1-B5.

The second variation considered is the distance of decline from stope location. Three different variations have been considered, i.e., 150 m (D1), 125 m (D2) and 100 m (D3) away from the stope location. Figures 4.11 – 4.13 show the different cases for distance of decline from stope location, i.e., 150 m, 125 m and 100 m, respectively.

The third variation considered is variation in stope dimension. Three different variation of stope dimension have been considered: [a] E1: 20 m (W) × 41 m (H), [b] E2: 30 m (W) × 41 m (H)

and [c] E3: 20 m (W) × 60 m (H). Figure 4.14-4.16 shows the different dimensions considered for the present study, i.e., case E1, E2 and E3, respectively. A total of 46 finite element models have been considered including the insitu model, based on the three different variations discussed above. In addition to these models, an insitu model has also been developed so as to compare the results of different cases analyzed.

Table 4.3 Different cases analyzed for the study

Cases	Description	Cases	Description
A1	2 adjacent primary stopes extracted from the centre	B5	9 extreme end primary stopes extracted towards the centre
A2	4 adjacent primary stopes extracted from the centre	C1	All the primary and secondary stopes extracted
A3	6 adjacent primary stopes extracted from the centre	D1	Average distance between decline and stope location is 150 m
A4	8 adjacent primary stopes extracted from the centre	D2	Average distance between decline and stope location is 125 m
B1	2 extreme end primary stopes extracted	D3	Average distance between decline and stope location is 100 m
B2	4 extreme end primary stopes extracted towards the centre	E1	Stope dimension: 20 m (W) × 41 m (H)
B3	6 extreme end primary stopes extracted towards the centre	E2	Stope dimension: 30 m (W) × 41 m (H)
B4	8 extreme end primary stopes extracted towards the centre	E3	Stope dimension: 20 m (W) × 60 m (H)

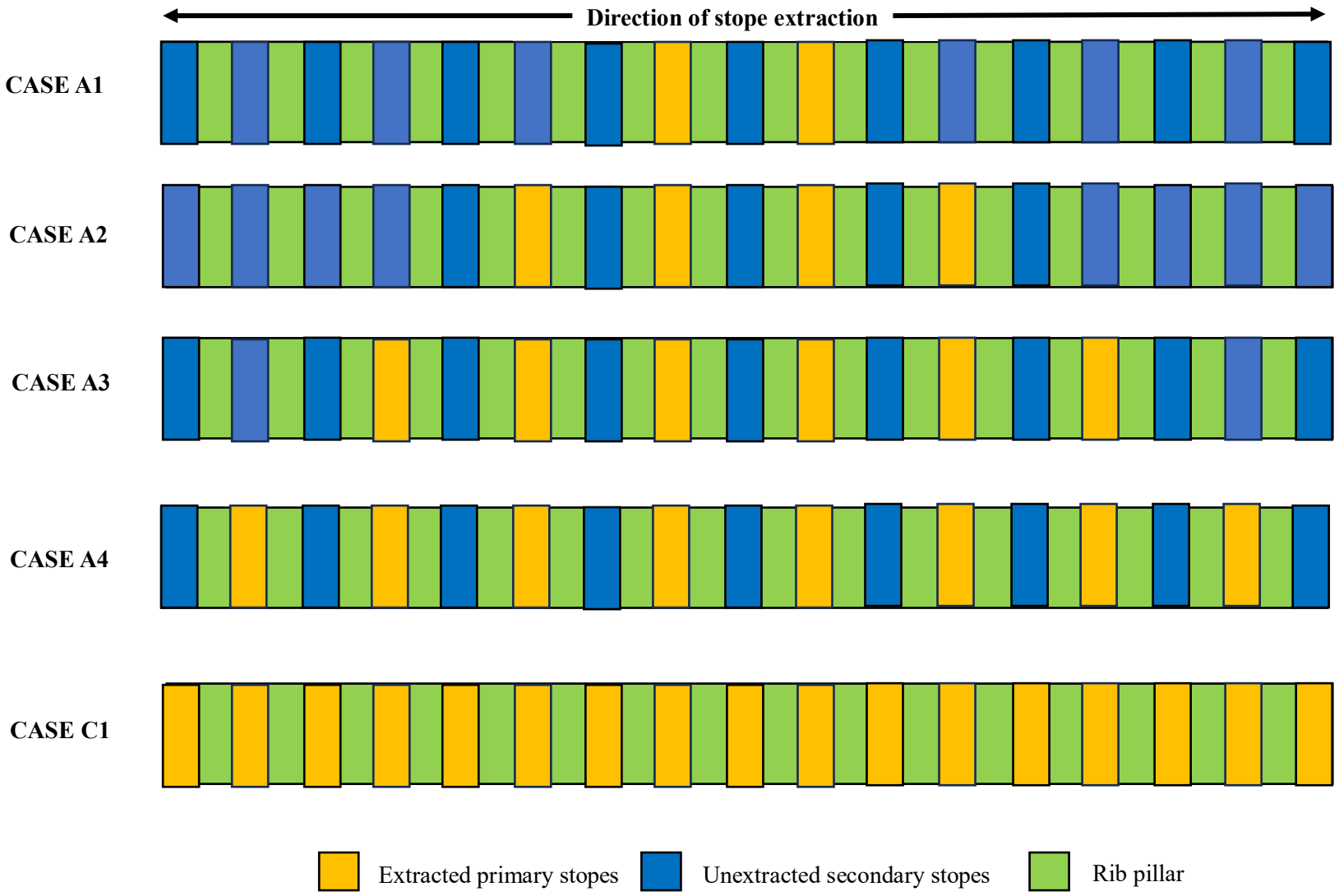

Figure 4.9 Schematic sketch of cases A1-A4 (Stope Extraction: from centre towards extreme end) and case C1 (All stopes extracted)

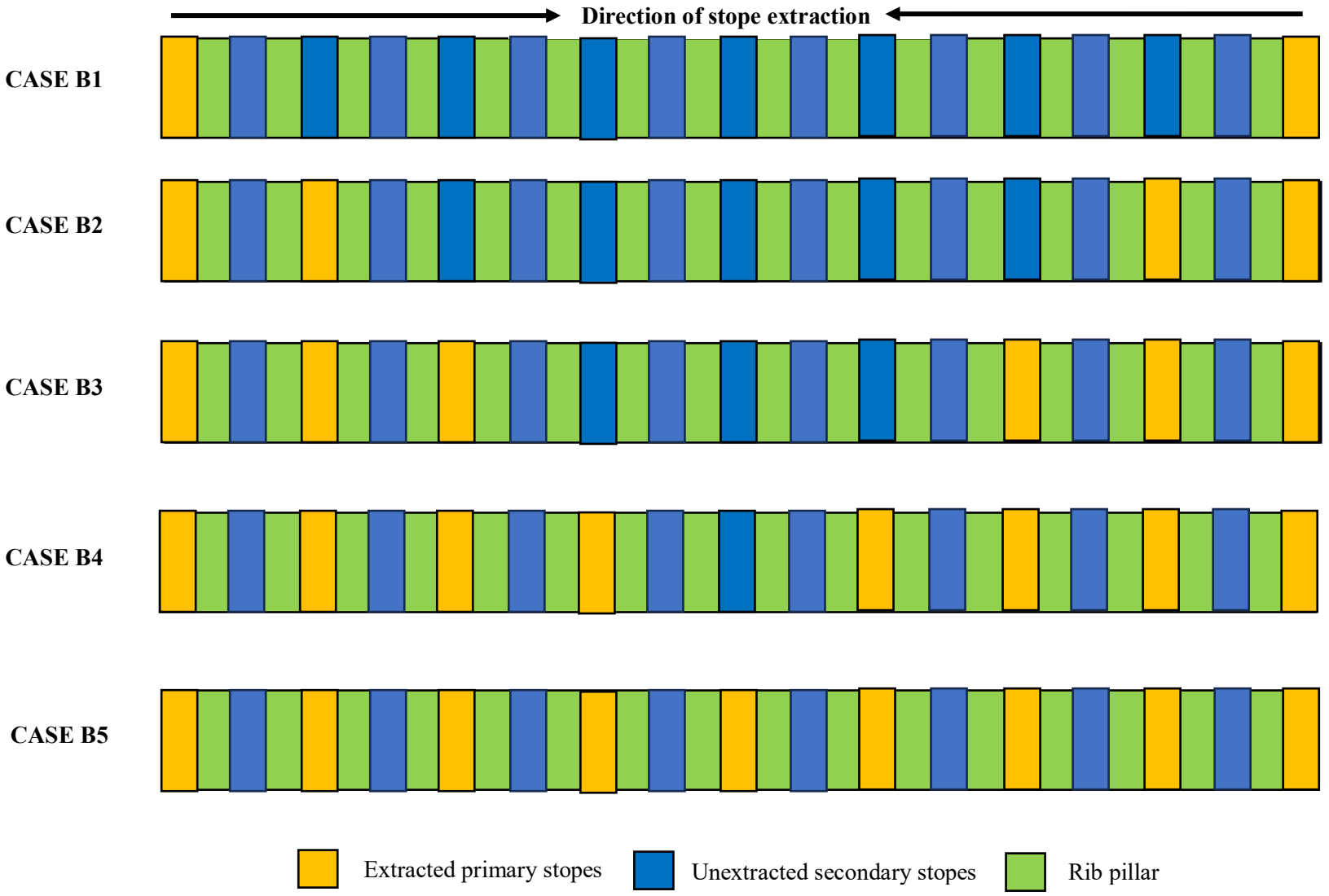

Figure 4.10 Schematic sketch of cases B1-B5 (Stope Extraction: Extreme end towards centre)

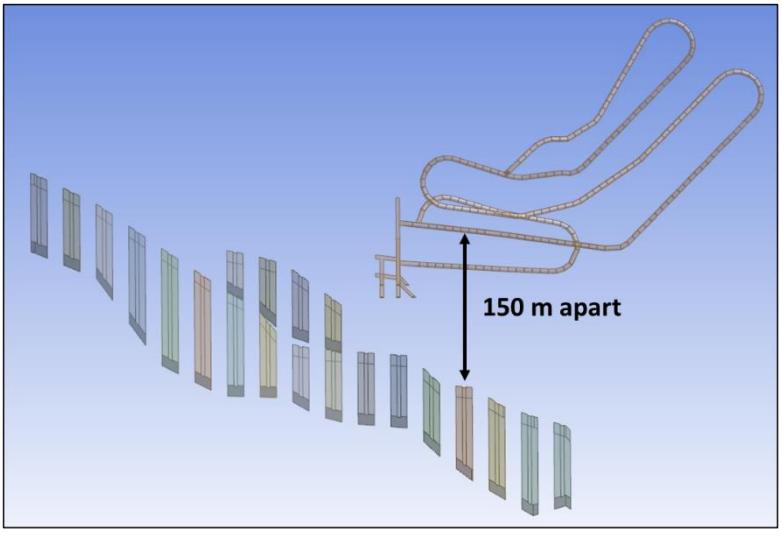

Figure 4.11 Case D1: Average distance of decline from production stopes: 150 m

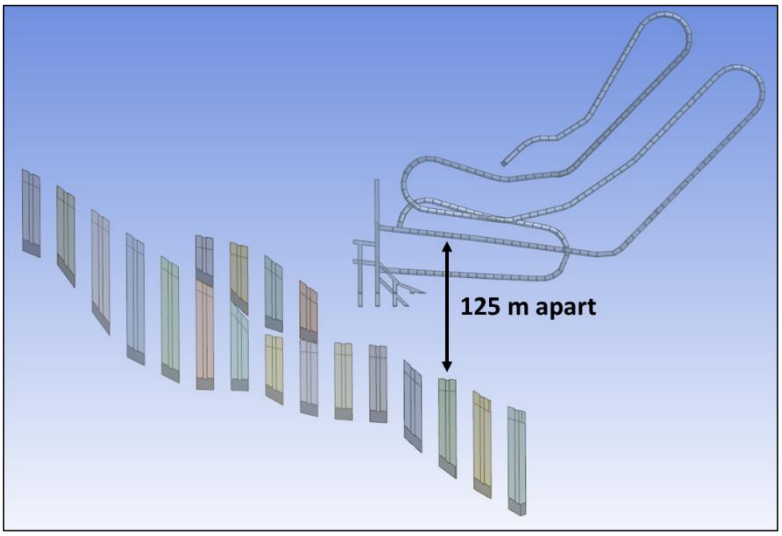

Figure 4.12 Case D2: Average distance of decline from production stopes: 125 m

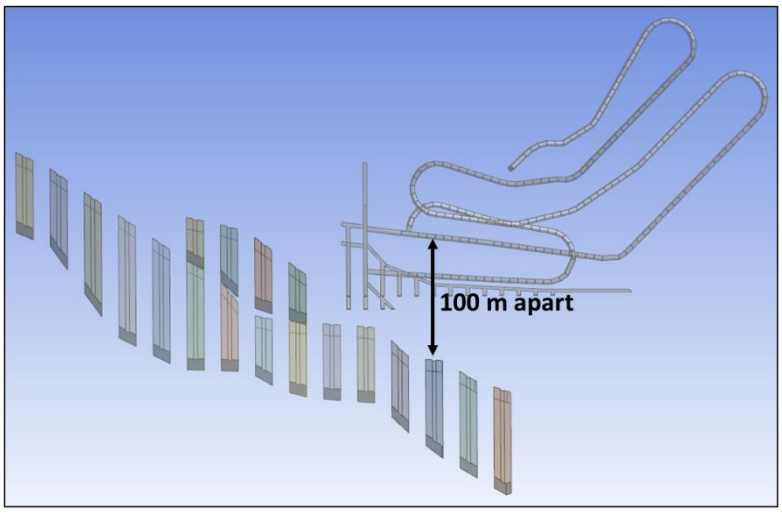

Figure 4.13 Case D3: Average distance of decline from production stopes: 100 m

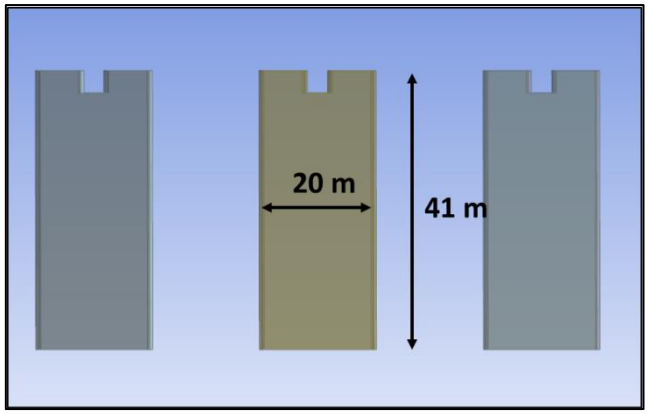

Figure 4.14 Case E1: E1: 20 m (W) × 41 m (H)

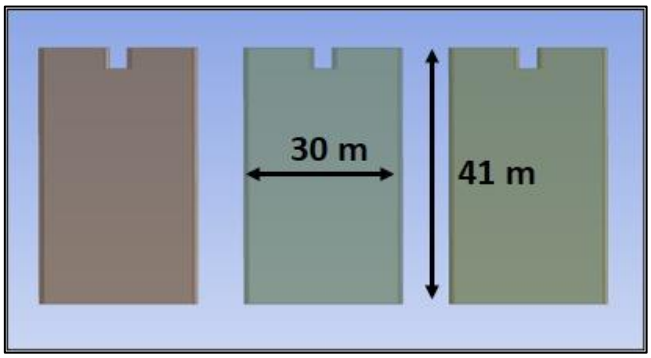

Figure 4.15 Case E2: E1: 30 m (W) × 41 m (H)

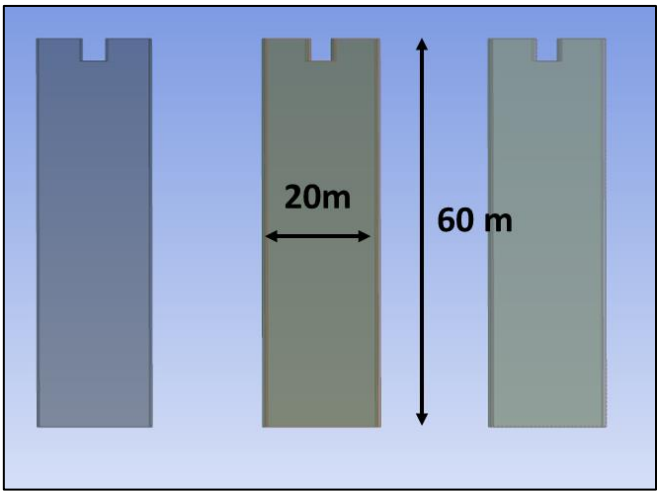

Figure 4.16 Case E2: E1: 20 m (W) × 60 m (H)

4.8 Pre-defined paths considered for the numerical analyses

Four different pre-defined paths, i.e., 1-4 have been considered for the numerical model to assess the stability of decline. Figure 4.17 shows the four predefined paths considered for the present study. Paths 1-4 are located at a distance of 0.5 m above the roof of decline so as to

analyze the effect of various parameters on the roof stability of the decline. The distance of 0.5 m is taken from the roof to closely analyze the behaviour of rock medium due to excavation.

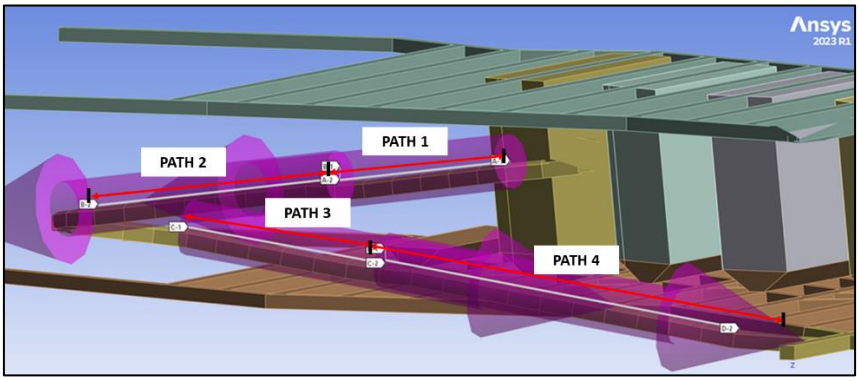

Figure 4.17 Predefined paths considered for the numerical model

4.8 Closure

The present chapter focused on the detailed description of the development of the three-dimensional finite element models of an underground hard rock mine below an open pit mine. Mesh convergence study has been carried out for 4 different element size and 4 m minimum element size has been considered for the simulation models so as to reduce the computational time. The loading and boundary conditions along with material properties and different cases analyzed have also been discussed in detail in this chapter.

Chapter 5: Results and Discussions

5.1 General

As discussed in chapter 4, three-dimensional numerical analyses have been developed for an underground hard rock mine operating below an open pit mine. The case study mine considered is Malanjkhand copper mine, where large diameter blasthole stoping method is adopted for extraction of ore. For the present study, the North mine of Malanjkhand copper project has been considered. Four different pre-defined paths have been considered, which are located 0.5 m above the roof of the decline and are at a distance of around 150 m from the first level stopes. Parametric study has also been carried out considering variation in dimensional parameters of the decline including cross-sectional shape and depth, rock-mass properties, stope design and stoping sequence and distance from the primary excavation zone. A total of 45 finite element models have been developed and analyzed including 1 insitu models (without any mining activity). The obtained simulation results are discussed in detail in this chapter.

5.2 Results of the numerical simulation

The results obtained from the numerical simulation models are evaluated in terms of factor of safety, maximum and minimum principal stress concentration factor and equivalent plastic strain. These results are assessed along path 1- 4 as discussed in section of chapter 4. The parameters considered for the study are discussed in detail as given below.

5.2.1 Effect of sequence of extraction

As discussed in chapter 4, two different sequences of extraction have been considered, i.e., centre to extreme end extraction and extreme end towards centre extraction for the first level stopes. A total of 10 different cases, i.e., A1-A4, B1-B5 and C1 have been considered as discussed in section 4.7. In the present study, the effect of sequence of primary stopes extraction on the decline stability has been analyzed along the predefined paths 1 - 4. The factor of safety plots for the different cases, i.e., A1-A4, B1-B5 and C1 have been analyzed along the predefined paths 1-4. Factor of safety (FoS) is defined as the ratio of strength of rock mass to induced stress at a point as a result of excavation. Figures 5.1 – 5.8 show the FoS plots along path 1 – 4 for different cases considered, respectively. It is observed that the maximum values

of FoS along paths 1 – 4 vary in the range of 1.5-2.6 for cases A1-A4 and 1.6-2.7 for cases B1-B5, respectively. The minimum values of FoS along paths 1 – 4 vary in the range of 1.1-1.25 for cases A1-A4 and 1.28 -1.45 for cases B1-B5, respectively. The FoS plot for the worst scenario, i.e., considering all primary and secondary stopes being extracted, are also plotted as shown in Figures 5.1 – 5.4.

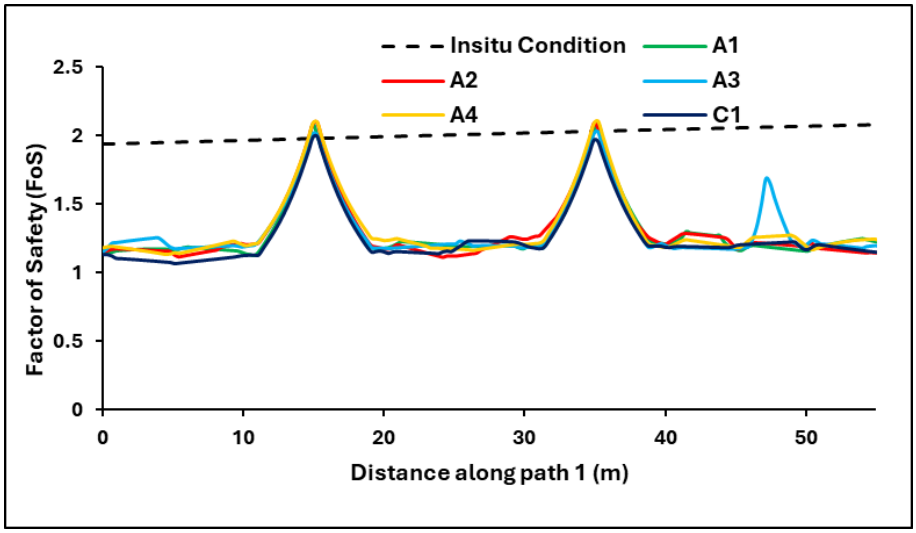

Figure 5.1 Factor of safety plots (A1-A4, C1) along path 1

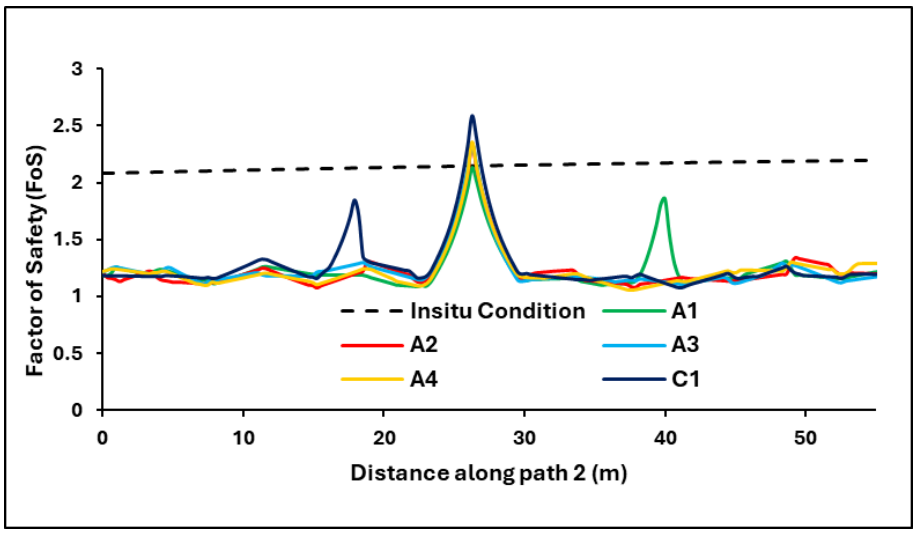

Figure 5.2 Factor of safety plots (A1-A4, C1) along path 2

From the plot, it can be observed that the average FoS value along path 1 for the different cases, i.e., A1-A4, B1-B5 and C1 are above unity, which clearly indicates that stope extraction in the first level has negligible effect on the stability of decline under given geo-mining conditions. The sudden increase in factor of safety values along the paths can be attributed to the presence of secondary stopes; whereas, there is sharp decrease in factor of safety values denote the adjacent excavation of the primary stopes. It should be also noted that for the numerical

simulation models, artificial supports used in the mines such as rock bolts, rock anchors, timber support, wire mesh etc. are not considered, which may further enhance the FoS values in the field.

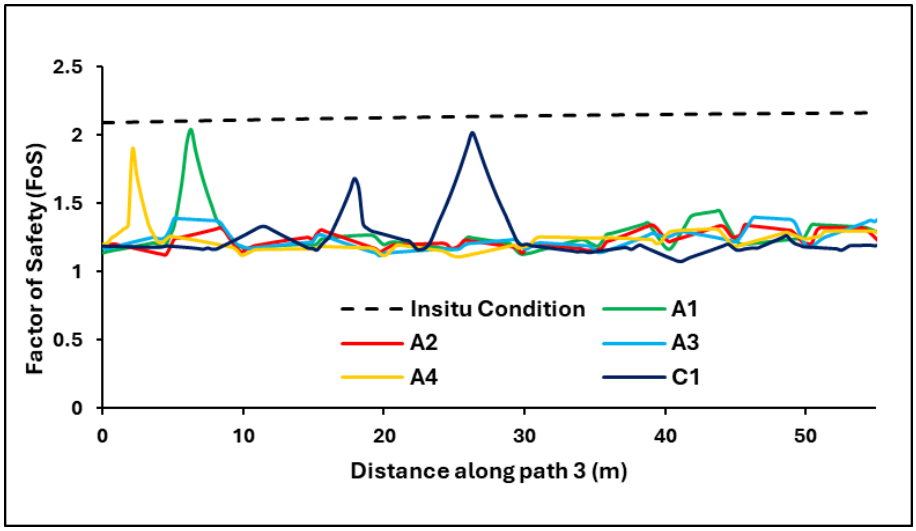

Figure 5.3 Factor of safety plots (A1-A4, C1) along path 3

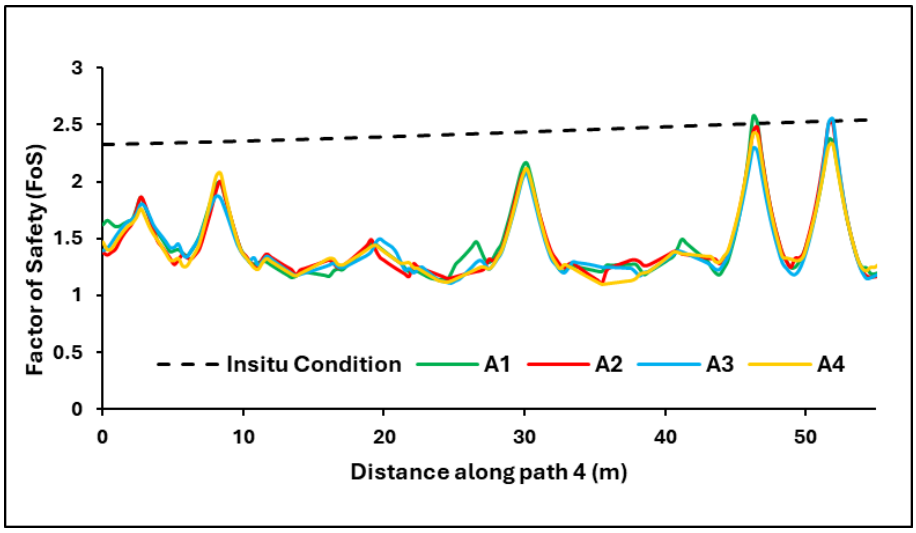

Figure 5.4 Factor of safety plots (A1-A4, C1) along path 4

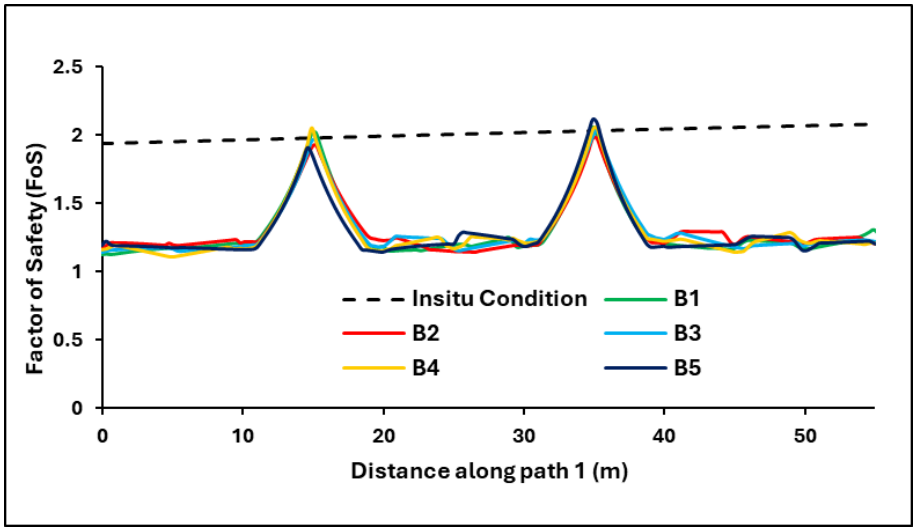

Figure 5.5 Factor of safety plots (B1-B5) along path 1

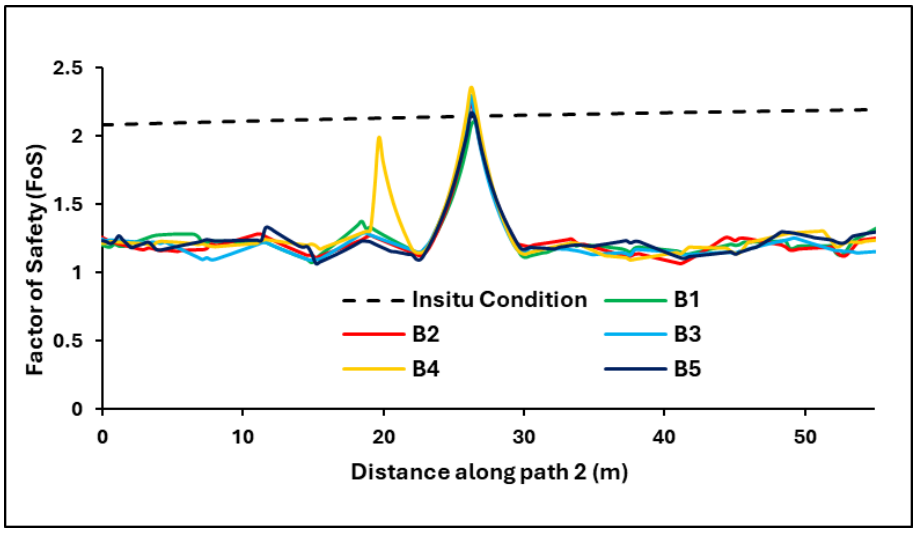

Figure 5.6 Factor of safety plots (B1-B5) along path 2

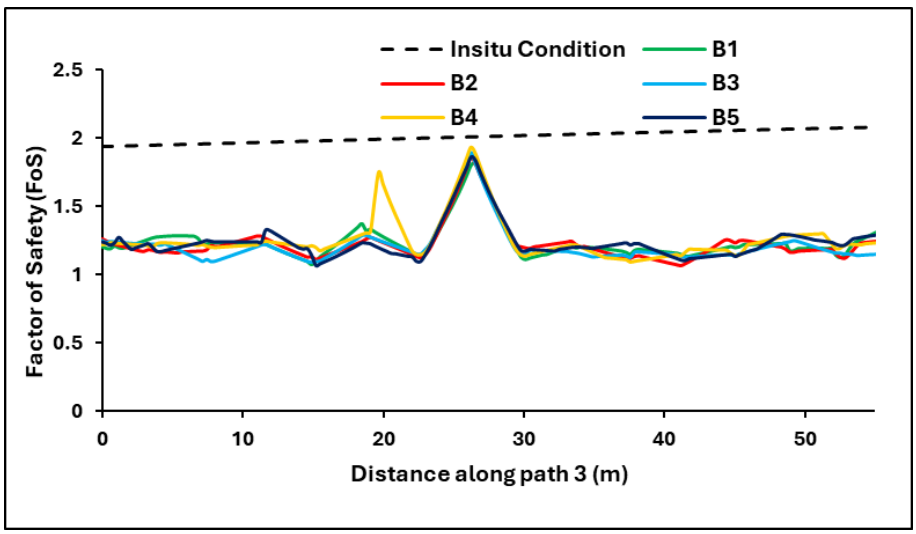

Figure 5.7 Factor of safety plots (B1-B5) along path 3

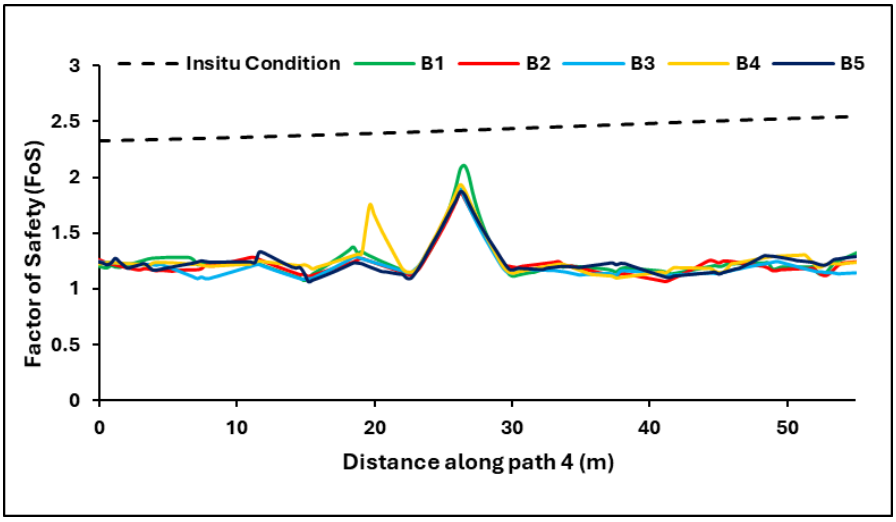

Figure 5.8 Factor of safety plots (B1-B5) along path 4

Stress concentration factor plots are also plotted along the predefined paths 1-4 for maximum and minimum principal stress values obtained from numerical simulation. Stress concentration factor is defined as the ratio of induced stress to insitu stress for given set of geo-mining condition. Figures 5.9 – 5.12 show the maximum principal stress concentration factors for the path 1-4, respectively. Whereas, figures 5.13-5.16 show the minimum principal stress concentration factors for the paths 1-4, respectively. From the plot, it can be observed that the maximum value of SCF vary in the range of 1.0-1.15; whereas, the minimum principal stress concentration factor varies in the range of 0.2-0.97. Similar observations are also seen for the different cases considered for the study. All the SCF values for path 1-4 are positive, which clearly indicates the stresses are compressive in nature and are also below the uniaxial compressive strength of the rock mass.

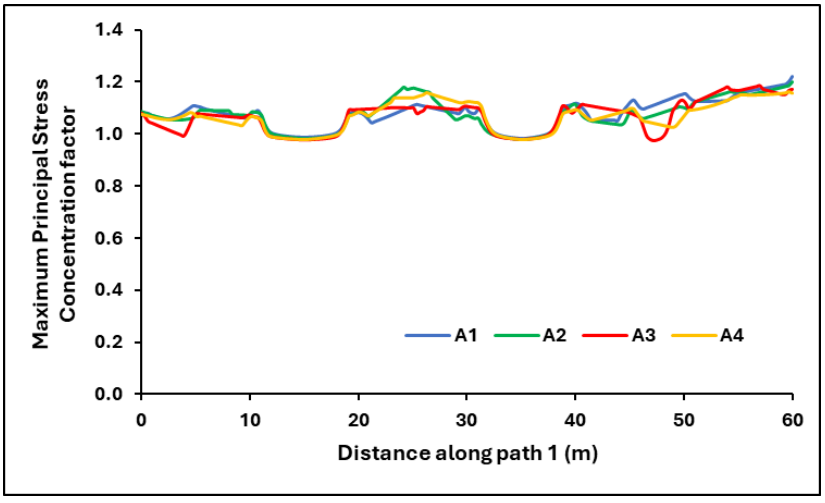

Figure 5.9 Maximum principal stress concentration factor plots along path 1

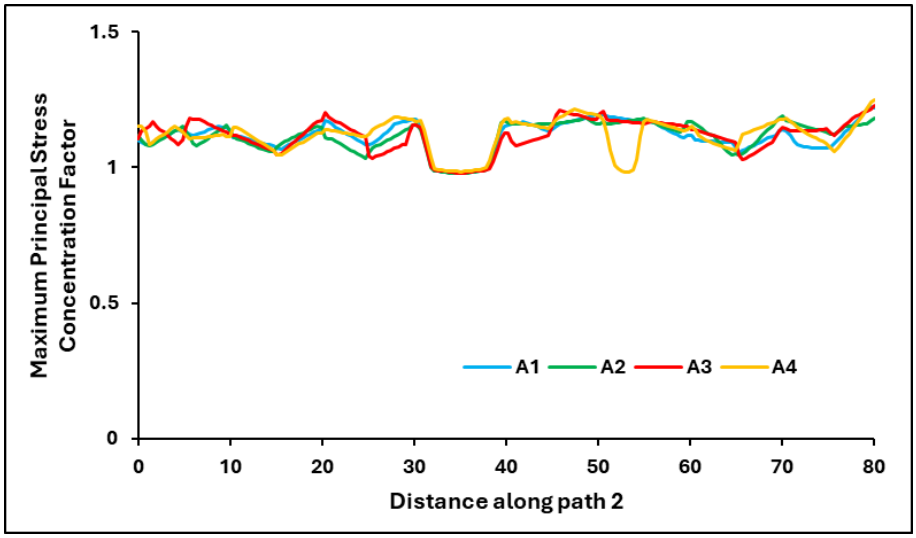

Figure 5.10 Maximum principal stress concentration factor plots along path 2

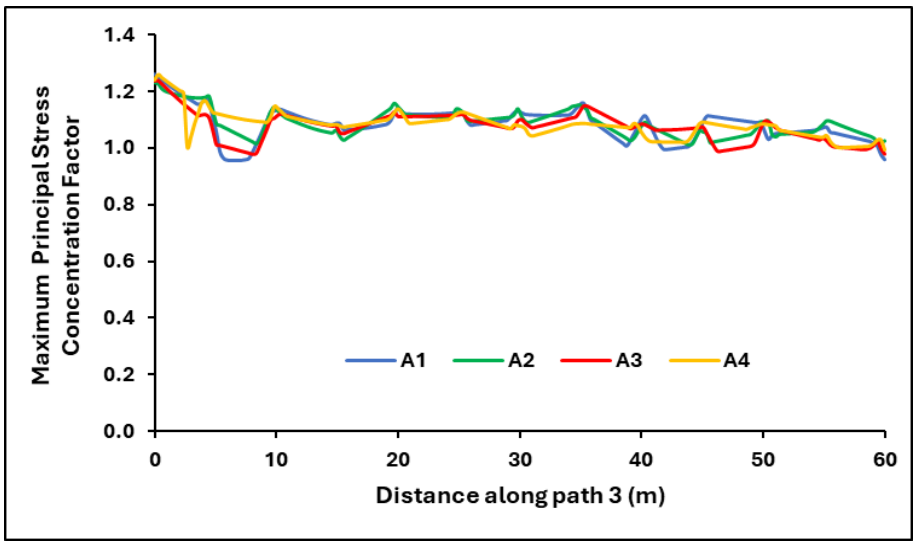

Figure 5.11 Maximum principal stress concentration factor plots along path 3

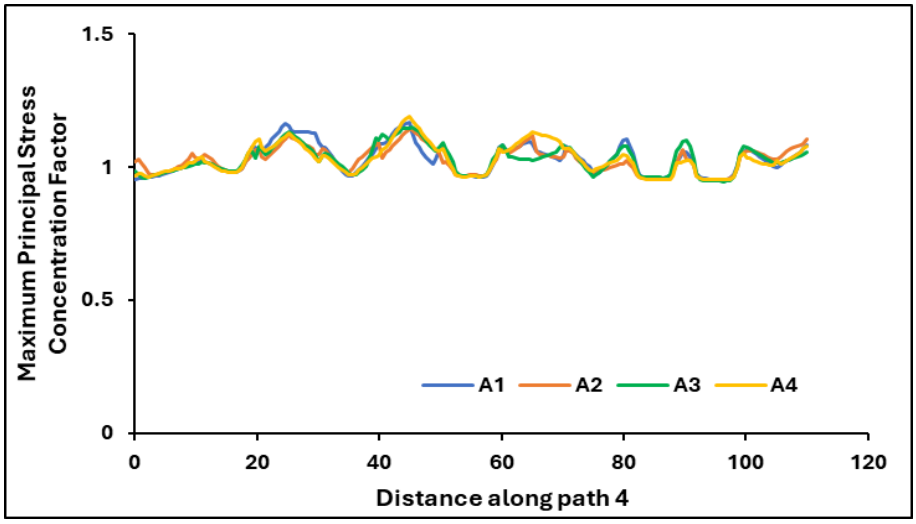

Figure 5.12 Maximum principal stress concentration factor plots along path 4

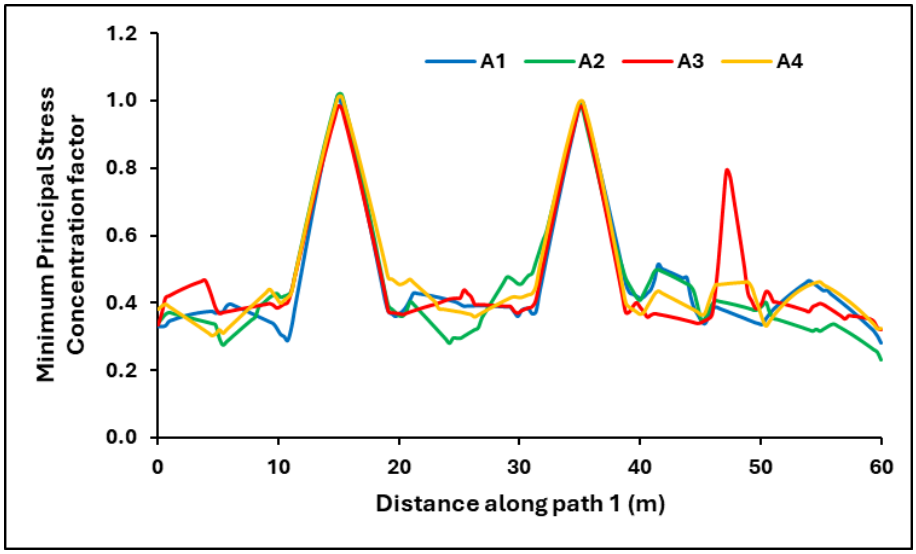

Figure 5.13 Minimum principal stress concentration factor plots along path 1

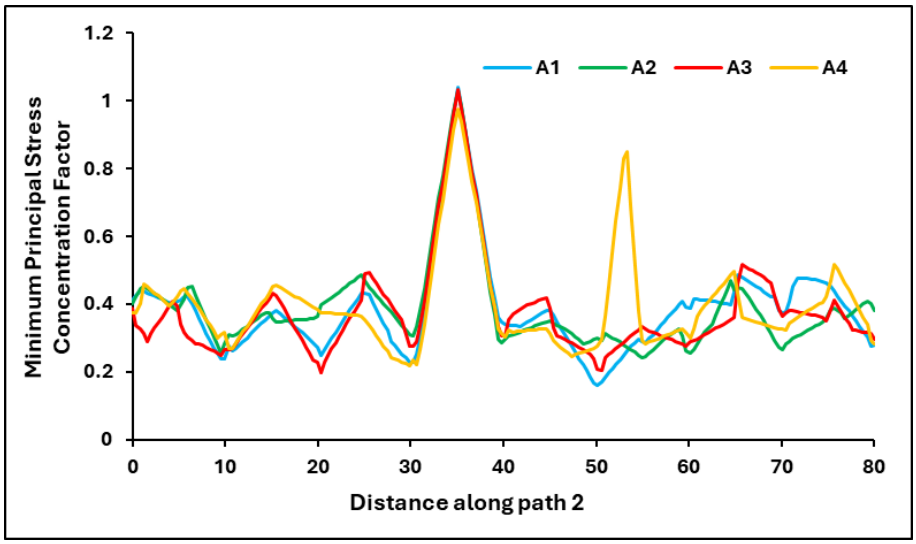

Figure 5.14 Minimum principal stress concentration factor plots along path 2

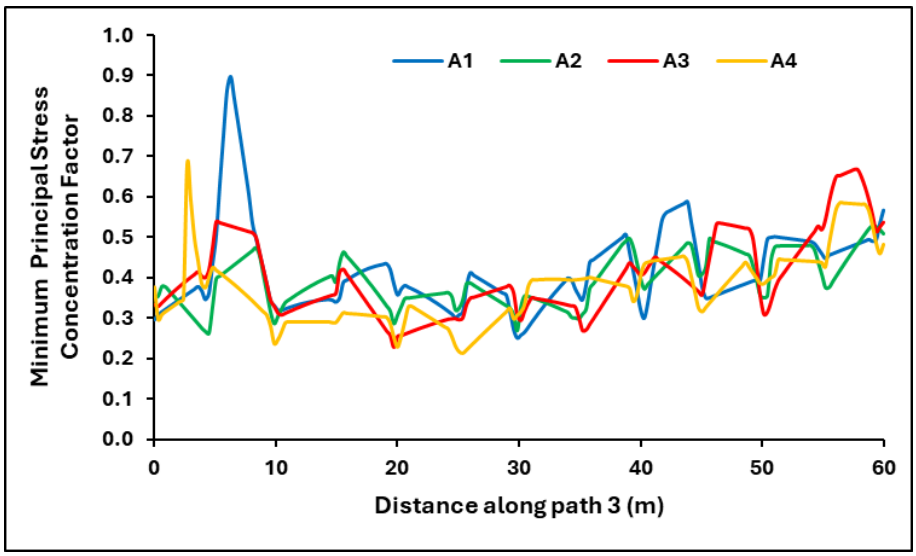

Figure 5.15 Minimum principal stress concentration factor plots along path 3

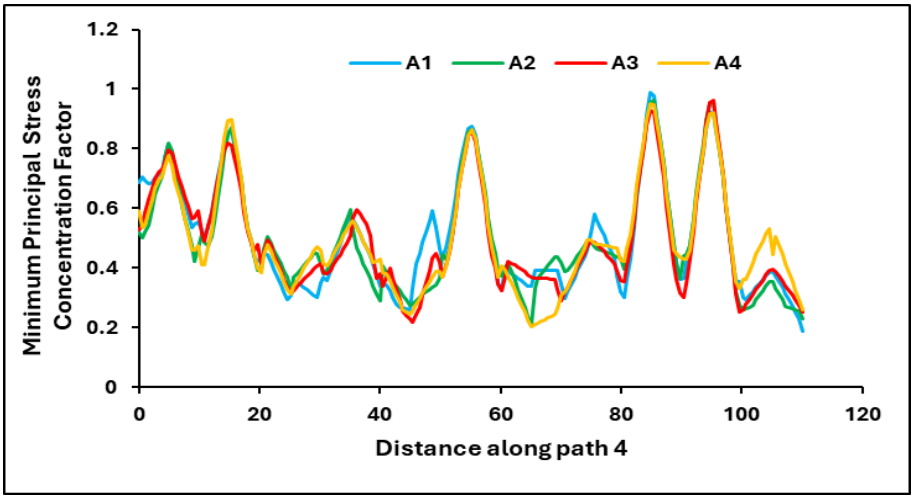

Figure 5.16 Minimum principal stress concentration factor plots along path 4

5.2.2 Effect of distance of decline from primary stope location

Three different variations in distance of decline from the stope boundary location, i.e., 150 m (D1), 125 m (D2) and 100 m (D3) have been considered in the present study as discussed in section 4.7. The factor of safety plots for the different cases, i.e., D1-D3 are carried out with respective to A1-A4, B1-B5, and C1 have been analyzed along the predefined paths 1-4. Figures 5.17 – 5.18 show the factor of safety plots along path 1 for cases A1 and A4, respectively; whereas, figures 5.19 – 5.20 show the factor of safety plots along path 1 for cases B1 and B5, respectively. Tables 5.1 – 5.2 show the average factor of safety values along path 3 and 4 for case A1, A4 and C1, respectively. From table 5.1, it is observed that for path 3, the average factor of safety varies in the range of 1.21-1.27 for Case D1; 1.36 – 1.42 for Case D2; and 1.19 – 1.27 for Case D3. From table 5.2, it is observed that for path 4, the average factor of safety varies in the range of 1.42-1.47 for Case D1; 1.50 – 1.68 for Case D2; and 1.39 – 1.44 for Case D3. Similar trend of observation is also found for Cases A2 and A3, respectively.

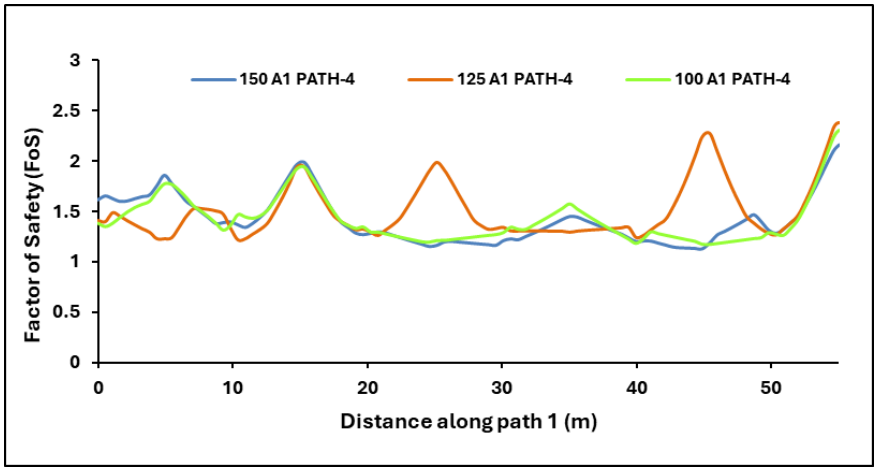

Figure 5.17 Factor of safety plots along path 1 for Case A1

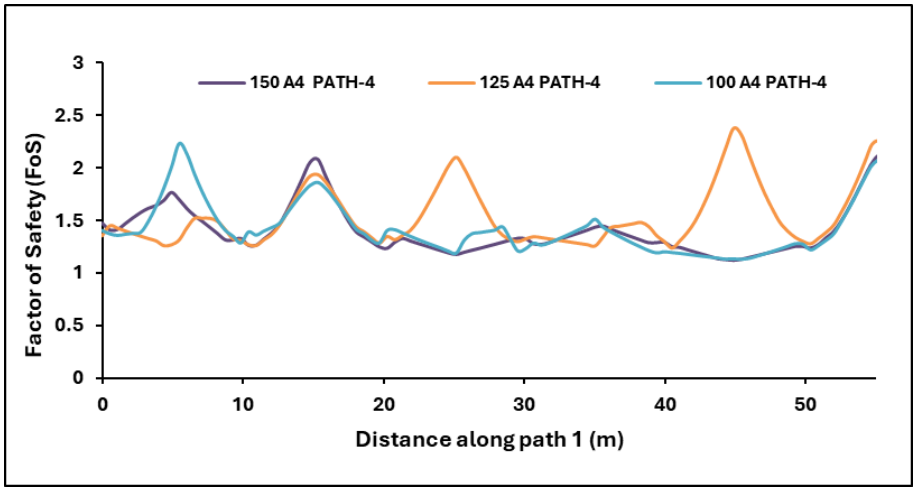

Figure 5.18 Factor of safety plots along path 4 for Case A4

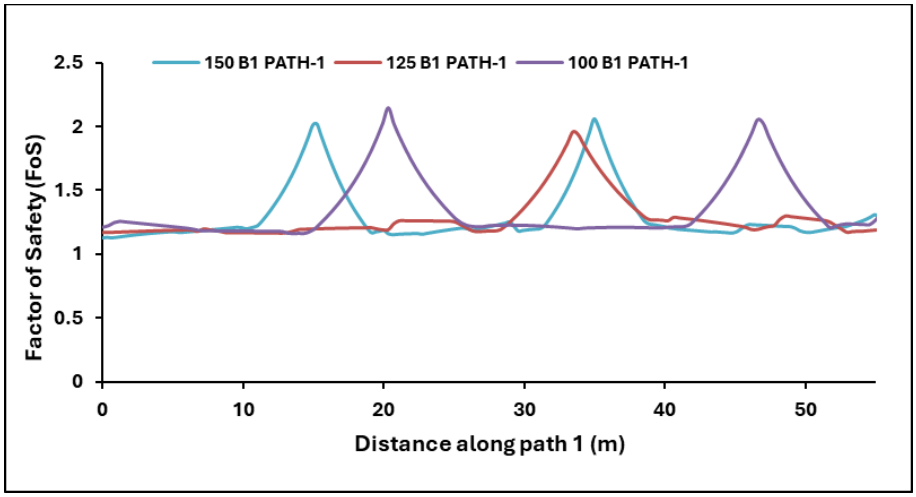

Figure 5.19 Factor of safety plots along path 1 for Case B5

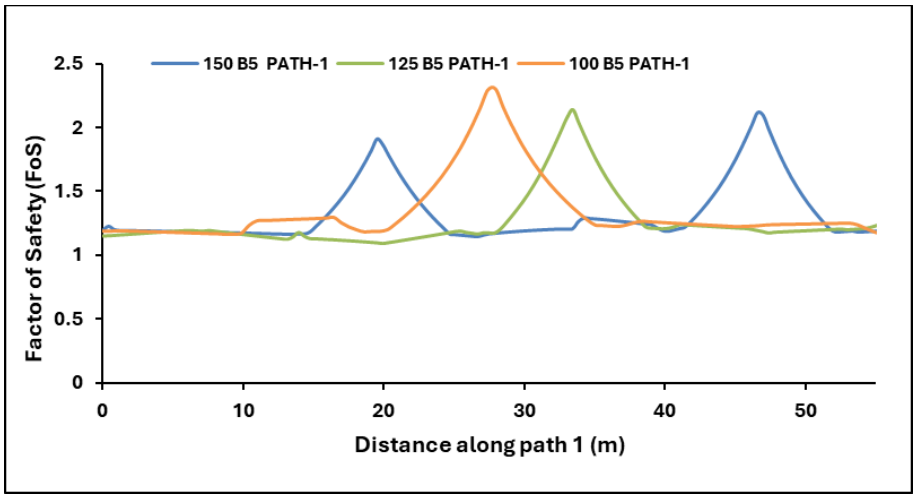

Figure 5.20 Factor of safety plots along path 1 for Case B5

Tables 5.3 – 5.4 show the average factor of safety values along path 1 and 2 for case B1 and B5, respectively. From tables 5.3 and 5.4, it is observed that for path 3 and 4, the average factor of safety varies in the range of 1.18-1.29 for Case D1; 1.32 – 1.56 for Case D2; and 1.22 – 1.31 for Case D3.

Table 5.1 FoS values for Cases A1, A4 and C1 for path 3

Sl No.	Distance between stopes and decline (m)	Case	Average FoS
1	150	A1	1.21
2	150	A4	1.29
3	150	C1	1.27
4	125	A1	1.42
5	125	A4	1.37
6	125	C1	1.36
7	100	A1	1.27
8	100	A4	1.22
9	100	C1	1.19

Table 5.2 FoS values for Cases A1, A5 and C1 for path 4

Sl No.	Distance between stopes and decline (m)	Case	Average FoS
1	150	A1	1.43
2	150	A4	1.42
3	150	C1	1.39
4	125	A1	1.50
5	125	A4	1.52
6	125	C1	1.68
7	100	A1	1.44
8	100	A4	1.43
9	100	C1	1.39

Table 5.3 FoS values for Cases B1 and B5 for path 1

Sl No.	Distance between stopes and decline (m)	Case	Average FoS
1	150	B1	1.29
2	150	B5	1.29
3	125	B1	1.56
4	125	B5	1.44
5	100	B1	1.31
6	100	B5	1.30

Table 5.4 FoS values for Cases B1 and B5 for path 2

Sl No.	Distance between stopes and decline (m)	Case	Average FoS
1	150	B1	1.23
2	150	B5	1.18
3	125	B1	1.34
4	125	B5	1.32
5	100	B1	1.25
6	100	B5	1.22

From the obtained data, it can be observed that when the average distance between the decline and stope boundary location on the footwall side is maximum, i.e., 150 m (Case D1), the average factor of safety varies in the range of for the different cases (A1-A4, C1 and B1-B5). With decrease in distance, i.e., 125 m (Case D2), there is slight increase in safety factor. The maximum percentage increase in average value of factor of safety for Case D2 as compared with Case D1 is around 13.42 %. However, as the average distance between the decline and stope location is further reduced to 100 m (Case D3), there is decrease in factor of safety as compared with Case D2 where the average distance is 125 m. The maximum percentage decrease in average factor of safety for Case D3 as compared with Case D2 are 11.4 % (Path 1-2). It can be attributed to the fact that for Case D1, though the distance between the decline and stope location on the footwall side is maximum, there exist effect of influence of open pit boundary which is close to the decline location. Similarly, for Case D3, the decrease in factor of safety values can be attributed to the effect of influence from the open stopes, drill crosscuts and other development drives which are near to the decline location. However, for Case 2, i.e., when the average distance maintained between the decline and stope location is 125 m, the effect of influence from both open pit boundary and production stopes is comparatively reduced; thereby, resulting in lower values of factor of safety as compared with Case D1 and D3.

5.2.3 Effect of change in stope dimension

Three different variations in stope dimensions have been considered for the present study including the existing dimension of stopes in the mines as discussed in section 4.7. In these three cases three variations with stope dimensions are considered which include E1: 20 m (W) × 41 m (H), E2: 30 m (W) × 41 m (H), and E3: 20 m (W) × 60 m (H) of stopes are analyzed conjunction with sequence of extraction. The width and height of stope are denoted by W and H, respectively. The factor of safety plots for the different cases, i.e., distances of increase in

stope width, increase in stope height, and original stope sizes are plotted and it is observed that carried out with respective to A1-A4, B1-B5, and C1 have been analyzed along the predefined paths 1-4. Table 5.5 shows the average value of factor of safety for cases A1, A4 and C1 along path 4. Table 5.6 shows the average value of factor of safety for cases B1 and B5 along path 1.

Table 5.5 FoS values for Cases A1, A4 and C1 for path 4

Sl No.	Stope Dimension	Case	Average FoS
1	E1:20 m (W) × 41 m (H)	A1	1.43
2	E1: 20 m (W) × 41 m (H)	A4	1.42
3	E1: 20 m (W) × 41 m (H)	C1	1.39
4	E2: 30 m (W) × 41 m (H)	A1	1.24
5	E2: 30 m (W) × 41 m (H)	A4	1.15
6	E2: 30 m (W) × 41 m (H)	C1	1.12
7	E3: 20 m (W) × 60 m (H)	A1	1.44
8	E3: 20 m (W) × 60 m (H)	A4	1.41
9	E3: 20 m (W) × 60 m (H)	C1	1.40

Table 5.6 FoS values for Cases B1 and B5 for path 1

Sl No.	Stope Dimension	Case	Average FoS
1	E1:20 m (W) × 41 m (H)	B1	1.39
2	E1: 20 m (W) × 41 m (H)	B5	1.32
3	E2: 30 m (W) × 41 m (H)	B1	1.19
4	E2: 30 m (W) × 41 m (H)	B5	1.17
5	E3: 20 m (W) × 60 m (H)	B1	1.35
6	E3: 20 m (W) × 60 m (H)	B5	1.36

From table 5.5, it is observed that for path 4, the average factor of safety varies in the range of 1.39-1.43 for Case E1; 1.12 – 1.24 for Case E2; and 1.40 – 1.44 for Case E3. From table 5.6, it is observed that for path 1, the average factor of safety varies in the range of 1.32-1.39 for Case E1; 1.17 – 1.19 for Case E2; and 1.35 – 1.36 for Case E3. Thus, it can be inferred that with increase in width of the stope, i.e., 20 m to 30 m, the average value of factor of safety decreases as compared with the general stope dimensions considered in the Malanjkhand mine. For cases B1 and B5, the maximum percentage decrease in factor of safety for Case E2 as compared with Case E1 is around 15.25 %. Increase in length of the stope height has also led to decrease in factor of safety values; however, the percentage decrease is almost negligible as compared with Case E2. For case B1 and B5, the maximum percentage decrease in factor of safety for Case E3 as compared with Case E1 is almost negligible, i.e., around 0.7 %. Similar trend has also been observed for Cases A1, A4 and C1 for factor of safety plots. For cases A1, A4 and C1, the maximum percentage decrease in factor of safety for Case E2 as compared with

Case E1 is around 15.25 %; whereas, there is no significant change in average factor of safety values for Case E1 and E3 considering paths 1-4.

5.3 Closure

The present chapter focused on the detail discussion of the results obtained from numerical simulation. A total of 45 different finite element models have been analyzed with variation in sequence of extraction, distance of decline from stope location on footwall side and stope dimensions. The results obtained were evaluated long four pre-defined paths 1-4 and some useful conclusions have been inferred from the study.

CHAPTER 6: CONCLUSIONS AND FUTURE SCOPE OF WORK

6.1 General

In the present study, three-dimensional finite element models are developed for an underground mine operating below an open pit mine. The case study mine considered is Malanjkhand copper mine, where large diameter blasthole stoping method is adopted for extraction of ore. The North mine of Malanjkhand copper project has been considered, where transverse method of ore extraction is carried out as the thickness of orebody is more than 20 m. Production from stopes is being carried out for the first level; whereas, the development work is in progress for the lower levels. The decline access is till the second level where development work is being carried out. The constitutive behaviour of the rock is modelled considering elastoplastic material properties. Parametric study is also carried out considering variations in dimensional parameters of the decline including cross-sectional shape and depth, rock-mass properties, stope design and stoping sequence and distance from the primary excavation zone. A total of 45 finite element models have been developed and studied considering 4 predefined paths, i.e., 1 -4, which is located 0.5 m above the roof of the decline. The results of the numerical simulations have been assessed in terms of factor of safety, maximum and minimum principal stress concentration factor and equivalent plastic strain.

6.2 Conclusions

Based on the results obtained from the numerical simulations, the following conclusions have been inferred:

1. Sequence of extraction has negligible effect on the stability of decline located at a distance of around 150 m from the primary stope location (orebody boundary). The average factor of safety for cases A1-A4, i.e., centre to extreme end extraction vary in the range of 1.12-2.05; whereas, the it varies in the range of 1.36 -2.15 for cases B1-B5, i.e., stope extraction from extreme end towards centre. For the worst scenario, i.e., case C1, where all the primary and secondary stopes have been extracted, there is no significant change in average safety factor along the predefined paths 1-4.

2. The distance of the decline from the stope location and also the open pit boundary plays crucial role in determining the stability of decline under considered geo-mining conditions. The maximum percentage increase in average value of factor of safety for Case D2 as compared with Case D1 is around 13.42 %. However, as the average distance between the decline and stope location is further reduced to 100 m (Case D3), there is decrease in factor of safety as compared with Case D2 where the average distance is 125 m. The maximum percentage decrease in average factor of safety for Case D3 as compared with Case D2 are 11.4 %.

3. The variation of dimension of the stopes considered for this study also affects the stability of decline to a certain extent. It is observed that increasing the width of the stope from 20 m to 30 m has led to decrease in factor of safety values by 15.25 % for Cases A1-A4 as compared with Case E1; whereas the maximum percentage decrease in factor of safety when the length of the stope is increased from 40 m to 60 m is around 0.07 %, i.e., nearly negligible. Similar trend has also been observed for Cases A1, A4 and C1 for factor of safety plots.

6.3 Future scope of work

The following are the future scope of work as mentioned below:

1. The present work can be further extended to lower levels of the mines with mining progressing downwards. Validation of the numerical simulation data can be carried out with the field data in future to check the efficacy of the simulation model.

2. The study can be further extended to analyze the effect of mining excavation on pillar stability including rib pillar, crown pillar, sill pillar and surface/barrier crown pillar.

3. Numerical modeling can be carried out considering dynamic analysis to incorporate the effect of production blasting on the existing underground structures. The effect of repeated blasting can also be analyzed as it may result in degradation of rock strength for the surrounding rock mass.

4. Artificial supports such as rock bolts, wire mesh etc. can be incorporated to analyze and study the effect of support system on the overall stability of the surrounding rock medium around the excavation opening.

References

- Zhao, R.-C., Tao, M., Zhao, H., Wu, C., & Cao, W. (2023). Theoretical study on dynamic stress redistribution around circular tunnel with different unloading paths. *Computers and Geotechnics*. https://doi.org/10.1016/j.compgeo.2023.105737
- Cai, X., Yuan, J., Zhou, Z., Pi, Z., Tan, L., Wang, P., Wang, S. S., & Wang, S. (2023). Effects of hole shape on mechanical behavior and fracturing mechanism of rock: Implications for instability of underground openings. *Tunnelling and Underground Space Technology*. https://doi.org/10.1016/j.tust.2023.105361
- Dashkovska, O. R. (2022). Stress analysis of an inclusion layer bonded to an irregularly shaped pore under an edge dislocation or a concentrated load. *Journal of Mechanics*, *38*, 397–409. https://doi.org/10.1093/jom/ufac028
- Svrkota, I., Milić, V., Petrovic, D., Djukanovic, D., & Denić, M. (2015). *Considerations on stability of open stopes in "Jama Bor" underground mine*. *27*, 31–39. https://doi.org/10.5937/PODRAD1527031S.
- Cai, M., Kaiser, P.K., and Tasdemir, M. (2004). "Characterization of stress and stability in deep mines." International Journal of Rock Mechanics and Mining Sciences, 41(2), 243-266
- Herget G. (1988) Stresses in Rock. Rotterdam, Balkema
- Kvapil R. and Blake W. (1973) Geometry and Stability determination of large dimension cut and fill rooms at Kamato. Proceedings of the Jubilee Symposium on Mine Filling. pp: 147-154
- Tavakoli M. (1994) Underground metal mine crown pillar stability analysis. University of Wollongong, (Research Online) Unpublished Thesis collections
- MOSHAB (1997) Geotechnical considerations in underground mines (Guidelines). Mines Occupational Safety and Health Advisory Board, Department of Industry and Resource, Western Australia. Document no: ZME723QT
- Edelbro C. (2003) Rock mass strength: a review. Department of Civil, Environmental and Natural Resources Engineering, Mining and Geotechnical Engineering. Luleå University of Technology. (Research Online) Unpublished Thesis collections
- Lu T. K., Guo B. H. and Cheng L.C. (2009) Review and interpretation of intersection stability in deep underground based on numerical analysis. Taylor and Francis Group. London. ISBN: 978-0-415-48475-6
- Gabriel S. E., Dennis R. D., John L.E and Leonard J. P., (2011) Pillar and roof span design guidelines for Underground Stone Mines. Department of Health and Human Services (NIOSH) Pittsburgh. Publication No. 2011-171
- Deb D. and Das K. C. (2011) Enriched finite element procedures for analyzing decoupled bolts installed in rock mass. International Journal of Numerical and Analytical methods in Geomechanics. Vol 35(15): 1636-1655
- Esterhuizen G.S. and Iannacchione A.T. (2011) Effect of the Dip and Excavation Orientation on Roof Stability in Moderately Dipping Stone Mine Workings. Department of Health and Human Services (NIOSH) Pittsburgh
- Kirsch G. (1898) The theory of elasticity and the needs of the strength of materials. Journal of the Association of German Engineers Vol 42: 797-807
- Evans W. H. (1941) The strength of undermined strata. Transactions of the Institution of Mining and Metallurgy. Vol 50: 475-532
- Adler L. and Sun M. C. (1968) Ground control in bedded rock formation. Bulletin 28, Research division. Virginia Polytechnic Institute. USA. pp: 42-74
- Wright F. D. (1972) Arching action in cracked roof beams. Fifth International Strata Control Conference. London. pp: 29-36
- Tavakoli Ladanyi B. (1974) Use of the long term strength concept in the determination of ground pressure on tunnel linings. Advances in Rock Mechanics. Proceedings of the 3rd Congress of the International Society of Rock Mechanics. Denver

- Brady B.H.G (1977) An analysis of rock behaviour in an experimental stoping block at Mt Isa mine, Queensland, Australia. International Journal of Rock Mechanics and Mining Sciences and Geomechanics. Abstract. Vol 14(2): 59-66
- Beer G. and Meek J. L. (1982) Design curves for roof and hanging walls in bedded rock based on Voussoir beam and plate solutions. Transactions of the Institution of Mining and Metallurgy. Vol 91: A18-A22
- Brady B, and Lorig L (1988) Analysis of rock reinforcement using finite difference methods. Computers and Geotechnics. Vol 5(2): 123-149
- Salamon M. D. G. and Munro. A. H. (1967) A study of the strength of coal pillars. Journal of the Southern African Institute of Mining and Metallurgy. Vol 68: 55-67
- Bieniawski Z. T. and Van Heerden W. L. (1975) The significance of in-situ tests on large rock specimens International Journal of Rock Mechanics and Mining Sciences. Vol 12: 101-113
- Hustrulid W. A. (1976) A review of coal pillar strength formulas. Rock Mechanics. Vol 8: 115-145
- Mark C. and Barton T. M. (1997) Pillar design and coal strength. Proceedings of the New Technology for Ground Control in Retreat Mining. US Department of Health and Human Services, Public Health Service, Centers for Disease Control and Prevention, National Institute for Occupational Safety and Health, Pittsburgh. Publication (No. 97–122). pp 49–59
- York G. (1998) Numerical modelling of the yielding of a stabilizing pillar/foundation system and a new design consideration for stabilizing pillar foundations. Journal of the Southern African Institute of Mining and Metallurgy. Vol: 98: 281-293
- Brady B. and Brown E. T. (2003) Rock mechanics for underground mining, 2nd edition. Chapman and Hall, London
- Mark C. (2006) The evolution of intelligent coal pillar design. Proceedings of the 25th International Conference on Ground Control in Mining. West Virginia University, Morgantown. pp: 325-334
- Mitri H. S. (2007) Assessment of horizontal pillar burst in deep hard rock mines. International Journal of Risk Assessment and Management. Vol 7(5): 695-707
- Jawed M., Sinha R. K. and Sengupta S. (2013) Chronological development in coal pillar design for bord and pillar workings: a critical appraisal. Journal of Geology and Mining Research. Vol 5(1): 1-11
- Hedley D. G. F. and Grant F. (1972) Stope and pillar design for the Elliot Lake Uranium mines, CIM Bulletin. pp: 37-44
- Von Kimmelman M. R., Hyde B. and Madgwick R.J. (1984) The use of computer applications at BCL Limited in planning pillar extraction and design of mining layouts. Proceedings of the ISRM symposium: design and performance of underground excavations. British Geotechnical Society, London. pp 53J63
- Krauland N. and Soder P. (1987) Determining pillar strength from pillar failure observation. Engineering and Mining Journal Vol 188 (8): 34-40
- Hudyma M. R. (1988) Rib pillar design in open stope mining. MSc Thesis. The University of British Columbia, Vancouver. Mining and Mineral Processing Engineering
- Potvin Y., Hudyma M. R. and Miller H. (1989) Design guidelines for open stope support. CIM Bulletin. Vol 82(926): 53-62
- Sjoberg J. (1992) Failure modes and pillar behaviour in Zinkgruvan mine. Proceeding of 33rd US symposium on Rock mechanics. Rotterdam. pp: 491-499
- Lunder P. J. (1994) Hard rock pillar strength estimation an applied empirical approach. University of British Columbia, Vancouver (MASc thesis)
- Lunder P. J. and Pakalnis R. (1997) Determination of the strength of hard rock mine pillars. Bulletin of Canadian Institute Mining and Metallurgy. Vol 90(1013): 51-55
- Maybee W. G. (1999) Pillar design in hard brittle rocks. Master's thesis, School of Engineering, Laurentian University, Sudbury, ON, Canada
- Laubscher D. H. (1977) Geomechanics classification of jointed rock masses – mining applications. Transactions of the Institutions of Mining and Metallurgy. Vol 86(1977): A1-A8

- Mathews K. E., Hoek E., Wyllie D. C and Stewart S. B. V. (1980) Prediction of stable excavation spans for mining at depths below 1000 meters in hard rock. Report to Canada Centre for Mining and Energy Technology (CANMET). Department of Energy Resources
- Diering J. A. C. and Laubscher D. H. (1987) Practical approach to the numerical stress analysis of mass mining operations. Transactions of the Institutions of Mining and Metallurgy. Vol 96: A179-A188
- Potvin Y. and Milne D. (1992) Empirical cable bolt support design. Proceedings of International Symposium on Rock Support. Balkema. Rotterdam
- Stewart S. B. and Forsyth W. W. (1995) The Mathew's method for open stope design. 95th CIM AGM. Calgary. Alberta. Vol 88(992): 45–53
- Hadjigeorgiou J., Leclaire J. and Potvin Y. (1995) An update of the stability graph method of open stope design. 97th Annual General Meeting. CIM. pp: 154-161
- Suorineni F. T., Tannant D. D. and Kaiser P. K. (1999) Fault factor for the stability graph method of open-stope design. Transactions of the Institutions of Mining and Metallurgy. Vol 108: A92–A104
- Trueman R., Mikula P., Mawdesley C. and Haries N. (2000) Experience in Australia with the application of the Mathews method of open stope design. CIM Bulletin. Vol 93(1036): 162–167
- Mawdesley C., Trueman R. and Whiten W. J. (2001) Extending the Mathews stability graph for open-stope design. Mining Technology. Vol 110(1): A27–A39
- Bewick R. P. and Kaiser P. K. (2009) Numerical assessment of factor B in Mathews' method for open stope design. Proceedings of the 3rd CANUS Rock Mechanics Symposium. Canadian Rock Mechanics Association. Toronto. ON
- Mitri H. S., Hughes R. and Zhang Y. (2011) New rock stress factor for the stability graph method. International Journal of Rock Mechanics and Mining Sciences. Vol 48: 141–145
- Chen D., Chen J. and Zavodni Z.M. (1983) Stability analysis of sublevel open stopes at great depth. The 24th U.S. Symposium on Rock Mechanics (USRMS)
- Martin C. D., Tannant D. D., Yazici S. and Kaiser P. K. (1999) Stress path and instability around mine openings. 9th ISRM Congress, Paris
- Zhang Y. and Mitri H. S. (2008) Elastoplastic stability analysis of mine haulage drift in the vicinity of mined stopes. International Journal of Rock Mechanics and Mining Sciences. Vol 45(4): 574-593
- Mortazavi A., Hassani F. P. and Shabani M. (2009) A numerical investigation of rock pillar failure mechanism in underground openings. Computers and Geotechnics. Vol 36: 691-697
- Wang Y. M., Huang M. Q., Wu A. X., Yao G. H. and Hu K. J. (2013) Rock Backfill and Hazard Control of Abandoned Stopes: A Case Study. Applied Mechanics and Materials. 3rd International Conference on Green Building, Materials and Civil. Vol 368-370(1): 1726-1731
- MOSHAB Trinh N. and Jonsson K. (2013) Design considerations for an underground room in a hard rock subjected to a high horizontal stress field at Rana Gruber, Norway. Tunnelling and Underground Space Technology. Vol 38: 205-212
- Abdellah W., Raju G. D., Mitri H. S. and Thibodeau D. (2014) Stability of underground mine development intersections during the life of a mine plan. International Journal of Rock Mechanics and Mining Sciences. Vol 72: 173-181
- Kumar H., Deb D. and Chakravarty D. (2017) Design of crown pillar thickness using finite element method and multivariate regression analysis. International Journal of Mining Science and Technology. Vol 27: 955-964
- Naung N., Sasaoka T., Shimada H., Hamanaka A., Wahyudi S. and Pisith M. (2018) Stability assessment of open stope under overlaying mined-out regions at Modi Taung gold mine, Myanmar. International Journal of Geosciences. Vol 9: 547-571
- Pariseau W.G. (1980) Finite element method applied in to cut and fill mining. Proceedings of International Conference on the Application of Rock Mechanics to Cut and Fill Mining, Sweden. pp: 197-204
- Wold M. B. (1980) Numerical stress analysis of post pillar mining at the Dolphin mine, King Island, stage 1: Parametric study Australia. CSIRO Division of Applied Geomechanics. Technical report. No TR111. pp: 42

- Sinclair T. J. E., Shillabeer J. H. and Herget G. (1981) Applications of a computer model to the analysis of rock – backfill interaction in pillar recovery operations. Application of rock mechanics to cut and fill mining. IMM. pp: 339-351
- Baria G. (1984) Stability studies of underground openings at the Masua mine, Sardinla, Italy. Design and Performance of Underground Excavations, ISRM Symposium, Cambridge, U.K. pp: 509-518
- Mitri H. S., Zhang L. and Fotoohi K. (1995). 3D finite element modelling of mine and fill sequences. CAMI'95: 3th Canadian Conference on Computer Applications in the Mineral Industry, Montreal
- Martin C. D. and Maybee W. G. (2000) The strength of hard-rock pillars. International journal of Rock Mechanics and Mining Sciences. Vol 37: 1239-1246
- Aubertin M., Li L., Arnoldi S., Belem T., Bussičre B., Benzaazoua M. and Simon R. (2003) Interaction between backfill and rock mass in narrow stopes. SoilRock2003: 12th Panamerican Conference on Soil Mechanics and Geotechnical Engineering, Cambridge, Massachusetts. USA
- Ferrero A., Segalini A. and Giani G. (2010) Stability analysis of historic underground quarries. Computers and Geotechnics. Vol 37: 476-486
- Gonen A. and Kose H. (2011) Stability analysis of open stopes and backfill in longhole stoping method for Asikoy underground copper mine. Article in Archives of Mining Sciences. Vol 56(3): 375-387
- Idris M. A., Saiang D. and Nordlund E. (2011) Probabilistic analysis of open stope stability using numerical modelling. International Journal of Mining and Mineral Engineering. Vol 3(3): 194-219
- Wang X., Kulatilake P. H. S. W. and Song W. (2012) Stability investigations around a mine tunnel through three-dimensional discontinuum and continuum stress analyses. Tunnelling and Underground Space Technology. Vol 32: 98–112
- Li X., Li D., Liu Z., Zhao G. and Wang W. (2013) Determination of the minimum thickness of crown pillar for safe exploitation of a subsea gold mine based on numerical modelling. International Journal of Rock Mechanics and Mining Sciences. Vol 57: 42–56
- Purwanto, Shimada H., Sasaoka T., Wattimena R. K. and Matsui K. (2013) Influence of stope design on stability of hanging wall decline in Cibaliung underground gold mine. International Journal of Geosciences. Vol 4: 1-8
- Kushwaha A., Himanshu V. K. and Sinha A. (2014) Design of stoping parameters and support system for longhole stoping method by numerical modelling. 5th Asian Mining Congress. The Mining Geological and Metallurgical Institute of India. Kolkata
- Yang Z., Zhai S., Gao Q. and Li M. (2015) Stability analysis of large-scale stope using stage subsequent filling mining method in Sijiaying iron mine. Journal of Rock Mechanics and Geotechnical Engineering. Vol 7: 87-94
- Himanshu V. K., Tiwari S., Kushwaha A. and Bhatacharjee R. (2017) Elasto-plastic failure analysis for design of stoping dimension in underground metalliferous mine. International Conference on NexGen Technologies for Mining and Fuel Industries. Pp 639-346
- Liu Z. X, Luo T., Li X., Li X. B., Huai Z. and Wang S. F. (2018) Construction of reasonable pillar group for undersea mining in metal mine. Transaction of Nonferrous Metals Society of China. Vol 28: 757-765
- Shnorhokian S., MacNeil B. and Mitri H. S. (2018) Volumetric analysis of rock mass instability around haulage drifts in underground mines. Journal of Rock Mechanics and Geotechnical Engineering. Vol 10: 60-71
- Mohanto S., and Deb D. (2020) Prediction of plastic damage index for assessing rib pillar stability in underground metal mine using multi-variate regression and artificial neural network techniques". Geotechnical and Geological Engineering.38(1), 767-90